Unifying Quantum Mechanics with Gravity, Demystifying Twenty Quantum Phenomena Including Half-Integer Spin, the Born Rule, Wave Function Collapse, and Higgs Physics

Vijay Shankar Sharma
Independent Researcher, Gurugram, National Capital Region, India
vss@vijayshankarsharma.com
ORCID: 0009-0001-9622-6121 DOI:
10.5281/zenodo.20145695
The author declares no conflict of interest and no funding was received for this research.

Abstract

This paper develops a physical account of quantum mechanics from the physical matter substrate that the author names the Spaticle field. The same matter substrate corresponds physically to what general relativity describes geometrically as spacetime. It has density, bends, compresses, waves, and becomes entrained by organised matter.

The adopted intrinsic equilibrium density is $\rho_s = 7.3 \times 10^{-27}$ kg/m³, derived in Paper 16 from the proton charge radius and condensation geometry. This density gives $\mu_s = 4.03358955 \times 10^{-27}$ m⁻¹, $L_s = 2.47918135 \times 10^{26}$ m = 26.205 Gly, $a_s = 1.20840317 \times 10^{-10}$ m/s², and $u_s = 6.5635567 \times 10^{-10}$ J/m³.

Gauge symmetry is interpreted as local circulation invariance of substrate condensations. The Schrödinger equation is recovered as the nonrelativistic, weak-field limit of the covariant carrier equation F1-cov. The Born rule describes the spatial distribution of successful irreversible interaction, wave-function collapse is physical state resolution during interaction, entanglement is a shared coherent substrate structure, and half-integer spin follows from the 720° restoration topology of organised condensations.

The observed H-class resonance is treated in BFUT as a radial resonance of the single Spaticle field. P19 derives $\lambda\_H\_vss = R_0/\pi^2$, $v\_vss = 6E\_unit/\alpha\_vss$, and $m\_H\_vss = v\_vss\sqrt{2\lambda\_H\_vss} = 124.75$ GeV/c². This derivation does not use the top-quark mass or a separate Higgs field.

The paper also examines measurement, decoherence, tunnelling, black holes, cosmological fine-tuning, and consciousness within the same substrate framework. The resulting account connects matter, forces, gravitation, quantum behaviour, propagation, and graded force-channel accessibility through one physical substrate and one consistent symbol system.

Keywords: quantum mechanics; Schrödinger equation; Born rule; gauge symmetry; spin statistics; Higgs boson; Spaticle field; matter substrate; wave-function collapse; entanglement; consciousness; configuration resonances

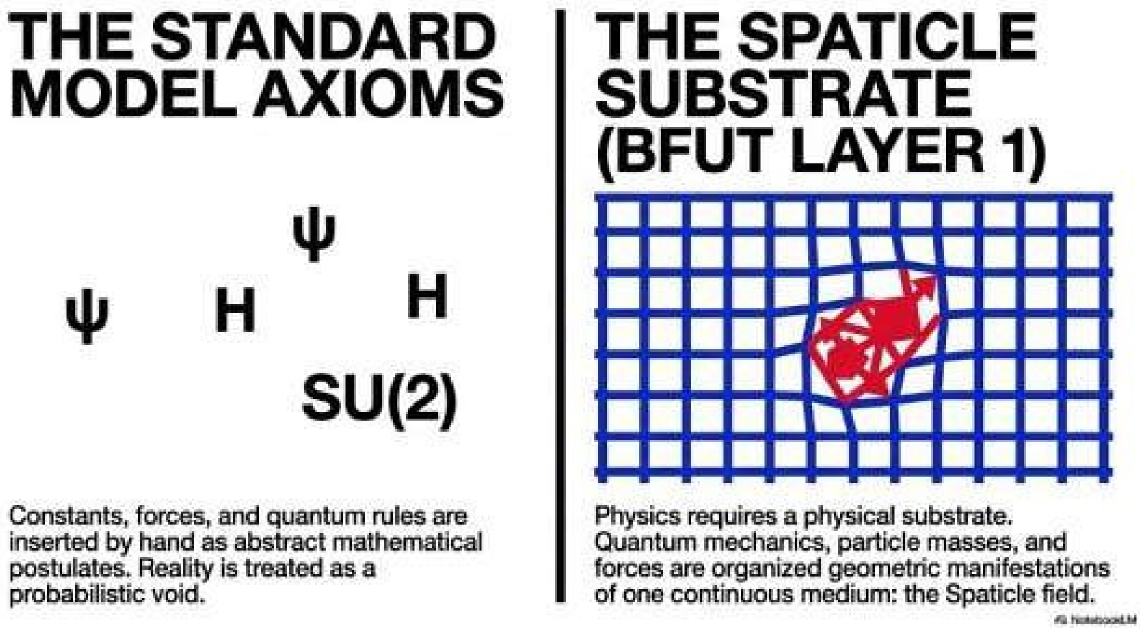

Figure 1: Standard Model axioms versus the BFUT Spaticle substrate framework.

Part I: Core BFUT Quantum and Physical Derivations

1. Introduction

Symbols and Notation Used in This Paper

ρ_s	Spaticle substrate equilibrium density	7.3×10^{-27} kg/m³
ħ_vss	BFUT-derived reduced Planck constant	1.055×10^{-34} J·s

m_p	Proton mass (SI anchor)	938.272 MeV/c^2
m_e_vss	BFUT-derived electron mass	0.511 MeV/c^2
F1-cov	Fully covariant carrier field equation	$g^{\mu\nu}\nabla_\mu\nabla_\nu(\delta\Psi) - \mu_s^2\delta\Psi = \kappa_s\nabla^2\Psi_{matter}$
R_d / DDR	Deformation domain radius	$R_d = (3M / (8\pi\rho_s))^{1/3}$
α_s_vss	Strong coupling constant	0.11785, 0.1179 (measured)
α_vss	Fine-structure constant	1/137.037, 1/137.036 (measured)
sin²θ_W_vss	BFUT electroweak mixing angle	$\sin^2\theta\_W\_vss = 1 - (m\_W\_vss/m\_Z\_vss)^2 = 0.23257$
m_H_vss	BFUT Higgs boson mass relation	$m\_H\_vss = v\_vss\sqrt{(2\lambda\_H\_vss)} =$ 124.75 GeV/c^2
m_t	Top quark mass	172.76 GeV
m_Z_vss	BFUT Z boson mass	91.396 GeV/c^2
m_W_vss	BFUT W boson mass	80.066 GeV/c^2
R_0	BFUT condensation equilibrium radius	1.27348221 (model units)
ℓ_model	BFUT model length scale from proton radius	$rp/R_0 = 6.607081 \times 10^{-16}$ m
λSI	SI substrate interaction parameter	$\rho_s/4 = 1.8257354 \times 10^{-27}$ kg/m³
y_t	Top Yukawa coupling	~1 (maximum substrate coupling)
E(R)	Free-energy functional for condensation	$A/R^2 + B\cdot R^2 + C\cdot R + D/R$
η	Propagation efficiency	$\eta = \sqrt{(1 - v^2/c^2)}$
DME	Dark-matter-effects law (P18)	$v^2(R)=v_b^2(R)[1+a_s R/v_b^2(R)]^{1/2}$; $a_s=c(G\rho_s/3)^{1/2}$
Ψ(r,t)	Spaticle carrier field / gravitational potential	Carrier field variable
δΨ	Carrier perturbation	$\delta\Psi = \Psi - \Psi_{vac}$
Ψvac	Vacuum equilibrium configuration	Equilibrium configuration of Ψ
λ_s	BFUT quartic Spaticle-field self-interaction coefficient	Fixed by selected field normalization
κ_s	BFUT source-to-substrate coupling coefficient	$\kappa_s = 1/c^2$
κ_vss	BFUT tunnelling	$\kappa\_vss = \sqrt{[2m(V-E)]}/\hbar\_vss$

	decay constant	
μ_s	BFUT carrier inverse-length response scale	$\mu_s = \sqrt{(3G\rho_s/c^2)}$ = $4.03358955 \times 10^{-27}$ m^{-1}
L_s	BFUT carrier response length	$L_s = 1/\mu_s = 2.47918135 \times 10^{26}$ m = 26.205 Gly
τc	Local carrier response / relaxation time	Lrlx = cτc
Lrlx	Carrier relaxation length	Lrlx = cτc
R_eff	Rotationally extended domain radius	R_eff = $R_d(1 + v_{rot}^2/c^2)^{1/3}$
m_eff	Effective rotational mass	m_eff = $M(1 + v_{rot}^2/c^2)$
a_s	Density-derived acceleration scale	$a_s = c^2\mu_s/3 = 1.20840317 \times 10^{-10}$ m/s^2
m*	Particle-sector mass scale	m* = m_e_vss/α_vss
r_e	Electron classical radius in BFUT chain	r_e = α_vss·ħ_vss/(m_e_vss·c)
u_g	Gravitational energy density	u_g = $Gm^{*2}/(8\pi r_e^4)$
u_s	Intrinsic substrate energy density	$u_s = \rho_s c^2 = 6.5635567 \times 10^{-10}$ J/m^3
G	Gravitational constant	6.67430×10^{-11} m^3 kg^{-1} s^{-2}
c	Speed of light / measured reference value	2.99792458×10^8 m/s
c	BFUT substrate propagation / numerical consistency result	2.99792458×10^8 m/s
r_p	Proton charge radius anchor	0.8414 fm
e	Elementary charge	$1.602176634 \times 10^{-19}$ C
ε_0	Vacuum permittivity	SI constant
k_e	Coulomb constant	$1/(4\pi\varepsilon_0)$
A, B, C, D	P16 free-energy coefficients	A=0.5, B=0.56308, C=−1/3, D=1
E(n)	P16 condensation energy for n units	−J·pairs(s) + λcond·Σ(s)^2 + (n−3)^2 + αgeom·(n−k) + D_s·cos(3φ)
J	P16 co-rotating pair binding coefficient	1.0
Σ	P16 circulation imbalance measure	$\Sigma(s) = \Sigma_i s_i$
λcond	P16 imbalance penalty coefficient	0.6

αgeom	P16 geometric imbalance coefficient	0.5
n	Number of condensation units	Integer count
k	Reference stable-unit count	k=3
D_s	P16 circulation phase reward coefficient	1.5
φ	P16 circulation phase angle	3+1: $\varphi=\pi/3$
ωc	Condensation circulation frequency	Used in circulation hierarchy
Q	Noether circulation occupancy	$i\int(\Phi^*\partial\Psi/\partial t - \Psi^*\partial\Phi/\partial t)d^3x$
Δx	Position uncertainty	Quantum localisation measure
Δp	Momentum uncertainty	Quantum localisation measure
p	Particle momentum	$p = \sqrt{(2m_eE)}$ in nonrelativistic examples
V	Potential energy	Barrier or external deformation energy
E	Particle energy	Total or incident energy as defined by context
T	Tunnelling probability	T = exp(−2κ_vss d)
d	Barrier width / tunnelling distance	Length
λ	de Broglie wavelength	λdB_vss = h_vss/p = 2πħ_vss/p
v_SM	Electroweak vacuum expectation value	≈246 GeV
θW	Weak mixing angle	The P19 mixing quantity is derived only after the independent W and Z resonance masses: $\sin^2\theta$_W_vss = 1 − (m_W_vss/m_Z_vss)^2 = 1 − $256^2/(9\pi^8)$ = 0.23257.
γ	Lorentz factor	$\gamma = 1/\eta$

The reconstruction of the Schrödinger equation and Born rule, the physical origin of half-integer spin, the 720° restoration topology, the Higgs-boson mass relation, observer-independent wave-function collapse, and the link between quantum mechanics and gravitation all follow from one physical matter substrate, which the author names the Spaticle field.

#	Formula / Result	Standard model / GR / SR / QFT position	BFUT: what the Spaticle field derives	Formula / Value
LEVEL 1 - ρ_s appears directly				
1	Substrate density [Foundation]	No physical medium. The vacuum is geometric spacetime. Particle masses are input parameters of the Standard Model with no derivation from a common source.	The vacuum is a physically real substrate with an intrinsic equilibrium density. The density anchors the carrier and large-scale branch; particle-sector masses follow the separate condensation-geometry chain.	$\rho_s = 7.3 \times 10^{-27}$ kg/m³
2	Nucleation energy functional [P16 Sec. 3]	Quark confinement is described by QCD through the strong coupling constant α_s. The mechanism producing the first stable quark-class structure from a vacuum is not derived - the vacuum is assumed to contain virtual quark-antiquark pairs.	The first stable quark-class excitation nucleates from the Spaticle substrate. Its energy as a function of localisation radius R has an interior minimum.	$E(R) = A/R^2 + B\cdot R^2 + C\cdot R + D/R$. Minimum at $R_0 = 1.27348$
3	Quark condensation radius [P16 Sec. 4]	The proton charge radius $r_p = 0.8414$ fm is measured. Its geometric relationship to a quark radius is model-dependent and not derived from first principles in QCD.	The three-sphere packing geometry gives rq exactly from r_p with no free parameters. One measured input. One derived output.	
4	Interstitial volume fraction [P16 Sec. 10]	No equivalent. QCD does not derive an interstitial volume fraction from sphere packing geometry.	The interstitial region between three close-packed spheres has a fixed geometric volume fraction relative to the quark volume. This is a pure geometric	

#	Formula / Result	Standard model / GR / SR / QFT position	BFUT: what the Spaticle field derives	Formula / Value
			constant.	
LEVEL 2 - one step from ρ_s: E_unit and the connecting identity				
5	Energy unit [P16 Sec. 4]	The proton mass m_p = 938.272 MeV is a measured input of the Standard Model. It is not derived from a substrate density or geometric principle.	At the actual ρ_s, mp is the measured SI anchor. The energy unit follows directly. A universe with different ρ_s would have a different E_unit scaling proportionally.	E_unit = mp·c² / π = 298.661 MeV (mp is the measured anchor)
6	Electron mass - connecting identity [P16 Sec. 10]	The electron mass m_e = 0.511 MeV is a measured parameter of the Standard Model. Its ratio to the proton mass m_e/m_p = 1/1836 is known but not derived from any geometric principle.	The electron mass follows from the interstitial geometry alone. E_unit cancels from both sides. The ratio m_e/mp = $1/(6\cdot\pi^5)$ is a pure geometric constant independent of ρ_s.	Egap / m_e = $6\cdot\pi^4$·Vgap/Vq = 45.00 [exact]. m_e = E_unit/$(6\cdot\pi^4)$ = 0.511009 MeV. m_e/mp = $1/(6\cdot\pi^5)$ [geometry only]
7	Interstitial gap energy [P16 Sec. 10]	No equivalent in QCD or the Standard Model.	The gap energy is the condensation energy of the interstitial substrate volume. It is the physical energy available for electron creation.	Egap = E_unit·Vgap/Vq = 298.661·0.0770 = 22.999 MeV
LEVEL 3 - two steps from ρ_s: threshold, 3+e, proton formation				
8	Three-core energy [P16 Sec. 6]	QCD describes three-quark binding through gluon exchange. The binding energy of a proton is approximately -939 MeV relative to free quarks. The mechanism is perturbative and non-perturbative QCD.	Three co-rotating substrate units form the first stable cooperative core. Energy computed directly from the condensation functional.	E(3-core) = 0.900 model units (full five-term functional, J=1.0, λ_{cond}=0.6, α_{geom}=0.5, D_s=1.5)
9	N=3+1 partition energy comparison [P16 Sec. 6]	QCD does not derive a partition energy comparison between symmetric and	At n=4 total units, partition energies confirm which arrangement is	4+0 = 6.10. 2+2 = 4.00. N=3+1 = 1.40 [preferred] (all model units)

#	Formula / Result	Standard model / GR / SR / QFT position	BFUT: what the Spaticle field derives	Formula / Value
		asymmetric quark arrangements from a free-energy functional.	preferred. N=3+1 decisively preferred over 4+0 and 2+2. This is a calculational result, not the physical proton.	
10	3+e state - proton formation [P16 Sec. 10]	The proton is a bound state of three quarks in QCD. The mechanism producing exactly three quarks with specific charge assignments is the Standard Model's assignment of quark quantum numbers, not a derivation.	The three-core generates its own electron through the 3+e mechanism. Energy drops from 0.900 to 0.8958. This is the physical proton-class structure. The electron is not a separate entity - it is created by the three-core.	E(3+e) = 0.8958 model units. ΔE = 0.0042 model units
11	Robustness of 3+e threshold [P16 Sec. 6.1]	QCD predicts proton stability through colour confinement. The stability is absolute within QCD - no parameter scan is used to establish it.	The 3+e preference holds across 97.56% of 1D, 95.95% of 2D, and 90.43% of 3D parameter space. Not a fragile result at a single tuned point.	1D: 97.56%. 2D: 95.95%. 3D: 90.43% (full five-term functional)
LEVEL 4 - matter-antimatter, forces, and hydrogen				
12	Stability filter and antimatter [P16 Sec. 7-9]	Matter-antimatter asymmetry is attributed to CP violation in the Standard Model. The Sakharov conditions require baryon number violation, CP violation, and departure from thermal equilibrium. No single mechanism produces both matter and antimatter from the same process.	The stability filter operates at formation. 90-97% of excitations stabilise as 3+e (matter). The remaining 2-10% are unstable excitations that collapse. The rebound is what physics calls the antiparticle. Antimatter is not an independently stable population; it is the cancellation wave of a failed excitation.	Stable 3+e (matter): 90-97%. Unstable collapse: 2-10%. Annihilation: complete (topology cancels exactly)
13	Matter-	Matter-antimatter	Matter and antimatter	3+e topology: (co-

#	Formula / Result	Standard model / GR / SR / QFT position	BFUT: what the Spaticle field derives	Formula / Value
	antimatter annihilation [P16 Sec. 8]	annihilation is described by QED and QCD via conservation of quantum numbers. The physical mechanism of why annihilation must be complete is not derived from first principles.	are circulation-topology inverses of the same substrate solution. When they meet, the circulations cancel exactly. Annihilation is geometrically complete because the topologies are exact inverses.	rotate, co-rotate, co-rotate). Inverse topology: (counter, counter, counter). Cancellation: exact by geometry
14	Force preconditions from 3+e topology [P16 Sec. 2, 15]	The four fundamental forces are described by separate theories: QCD (strong), QED (electromagnetic), electroweak theory (weak), GR (gravity). No single mechanism derives all four from one substrate topology.	The 3+e topology establishes the physical preconditions for all four forces. Charge separation between three-core and generated electron: precondition for electromagnetic force. Three-sphere packing geometry: precondition for strong confinement. Stability filter asymmetry: precondition for weak force asymmetry. Substrate deformation: precondition for gravity.	EM: charge separation in 3+e. Strong: three-sphere confinement. Weak: stability filter asymmetry. Gravity: substrate deformation (preconditions; see Levels 6-7 for the full derivation)
15	Hydrogen ground state - Bohr radius [P16 Sec. 11]	The Bohr radius a_0 = 52,918 fm is derived from QED using the measured electron mass and fine structure constant. It is not derived from a substrate density.	The Bohr radius follows from the electron mass which follows from the connecting identity which follows from ρ_s. A universe with different ρ_s would have atoms of different size.	$a_0 = \hbar^2/(m_e \cdot ke \cdot e^2)$ = 52,918 fm. a_0 proportional to ρ_s^{-1}
16	Hydrogen	The hydrogen ground	The binding energy	EH = -13.6 eV = -

#	Formula / Result	Standard model / GR / SR / QFT position	BFUT: what the Spaticle field derives	Formula / Value
	binding energy [P16 Sec. 11]	state energy -13.6 eV is derived from QED. It is not connected to a substrate density.	follows from m_e which follows from ρ_s. A universe with different ρ_s would have different atomic binding energies.	$m_e \cdot ke^2 \cdot e^4/(2 \cdot \hbar^2)$. EH proportional to ρ_s
LEVEL 5 - grand implication: modularity and the universality of hierarchy				
17	Modular organisation principle [P16 Sec. 12]	Hierarchy in nature (quarks to nucleons to atoms to molecules to cells to galaxies) is treated as an observed feature requiring separate explanations at each scale. No single principle derives hierarchy from energy minimisation.	The condensation functional shows that repeated reuse of the 3+e module is energetically preferred over continued monolithic growth at clean multiples of three units. The energy advantage at clean multiples grows with system size.	E_{single} grows superlinearly. $E_{modular}$ = floor(n/3)·0.8958 + $E_{remainder}$. Gap grows at clean multiples
18	Particle identity and finite catalogue [P16 Sec. 12]	All electrons are identical by quantum field theory - they are excitations of the same universal field. The number of stable particles is an experimental observation. No derivation of why exactly these particles are stable is offered.	Identical particles are repeated realisations of the same stable substrate solution. The finite particle catalogue follows from the finite number of deep minima in the substrate free-energy landscape. At n=4 exactly three configurations exist; 3+e dominates.	$m_e/mp = 1/(6 \cdot \pi^5)$ [pure geometry, ρ_s cancels]. Stable configurations at n=4: 3+e: 97.56%. 2+2: 2.16%. 4+0: 0.28%
19	Atom size fixed by ρ_s [P16 App. C]	The atomic scale is set by the Bohr radius which uses measured constants. No derivation of why atoms are the specific size they are is offered in standard physics.	Atom size is a derived consequence of ρ_s. If ρ_s doubled, atoms would be half the size. The actual atom size follows from the substrate density through the connecting identity chain.	mp proportional to ρ_s. m_e proportional to ρ_s. a_0 proportional to ρ_s^{-1}. EH proportional to ρ_s. m_e/mp = constant [geometry]

#	Formula / Result	Standard model / GR / SR / QFT position	BFUT: what the Spaticle field derives	Formula / Value
LEVEL 6 - forces emerge from the 3+e topology [P17]				
20	Gravity as substrate restoring response [P17 Sec. 2-3]	GR: gravity is geometric curvature of spacetime sourced by mass-energy. No mechanical mechanism is given for why mass curves spacetime.	Gravity is the Spaticle substrate's own mechanical restoring response to deformation by mass, and not an externally imposed geometric feature. Connects directly to the covariant carrier equation validated in P18.	Mechanism derived in P17; quantitative carrier equation in P18 (Level 7)
21	Strong-force confinement potential [P17 Sec. 5.2 / P19 Sec. 20.6]	QCD: confinement modelled through colour charge and gluon exchange. The string tension (~0.9 GeV/fm) is measured, not derived from a substrate.	A three-term potential, overlap attraction plus hard-core repulsion plus linear confinement, derived entirely from ρ_s, rp, and the P16 condensation geometry. No new free parameters.	$C_s = F_{conf} = 0.574$ GeV/fm vs measured 0.9 GeV/fm. Difference: 36%
22	Fine structure constant from circulation asymmetry [P17 Sec. 6.8 / P19]	QED: α = 1/137.036 is measured; no physical mechanism derives its value.	$\alpha = \omega_c^2 \cdot \chi_{rot} / (4 \cdot \pi \cdot c)$, with ω_c set by the D coefficient of the P16 functional and χ_{rot} the rotational polarisability at the condensation boundary.	α = 1/137.037 vs 1/137.036. Difference: 0.00048%
23	Weak mixing angle and parity violation [P17 Sec. 7.3 / P19 Sec. 6]	Electroweak theory: sin²(θ_W) = 0.2312 is measured. Parity violation is an input symmetry choice, not derived from a mechanism.	The BFUT electroweak mixing quantity is an output of the independently derived W and Z resonance masses; it is not an input to either mass.	$\sin^2\theta\_W\_vss = 1 - (m\_W\_vss/m\_Z\_vss)^2 = 1 - 256^2/(9\pi^8) = 0.23257$.
24	Electron-capture / neutron-formation	Standard Model: electron-capture threshold 0.782 MeV = $(mn - m_p - m_e)c^2$ is	The threshold is the dominance-inversion point at which the electron unit's	0.782 MeV (dominance-inversion threshold)

#	Formula / Result	Standard model / GR / SR / QFT position	BFUT: what the Spaticle field derives	Formula / Value
	threshold [P17 Sec. 7.4D]	measured; not connected to a substrate mechanism.	rotational energy density exceeds the three-core's rest-mass substrate deformation, set by ρ_s, rp, and the expelled mass fraction μ.	
LEVEL 7 - unified gravitation, rotation curves, and gravitational waves [P18]				
25	Effective local carrier field equation, F1 [P18 Sec. 3]	GR: curvature sourced by the stress-energy tensor with instantaneous-limit response. Newtonian gravity: action treated as instantaneous.	A single covariant carrier equation with a finite response time τ_c. GR and Newtonian gravity are recovered as settled-domain approximations as τ_c -> 0.	
26	Carrier relaxation timescale [P18]	GR / Newtonian gravity: no relaxation time; gravitational response is instantaneous (Newtonian limit) or exactly luminal (GR).	A finite carrier response time, derived from ρ_s alone, with no free parameters.	τ_c and $L_{rlx} = c\tau_c$ are local transient-response quantities; no universal fixed value is assigned.
27	Finite gravitational domain radius, DDR [P18]	Lambda-CDM: dark matter halo profile (e.g. NFW) fitted per galaxy with two or more free parameters.	Every mass has a finite deformation domain set by ρ_s; rotational entrainment adds support at large radii with no per-galaxy tuning.	$Rd = (3M/(8\cdot\pi\cdot\rho_s))^{1/3}$. $Reff = Rd\cdot(1+vrot^2/c^2)^{1/3}$
28	175 SPARC galaxy rotation curves [P18]	Lambda-CDM/NFW: halo parameters fitted per galaxy. MOND: one fitted acceleration scale a_0.	DME uses one a_s from ρ_s. No per-galaxy gravity parameter.	Shape 92.0%, flat 98.8%, median outer residual 0.096
29	KiDS-1000 weak gravitational lensing [P18]	Standard NFW halo profile fitted per stellar-mass bin.	Same DME equation and the same a_s as SPARC.	Same a_s on isolated-lens stacks
31	Spaticle field as the physical	Lambda-CDM: dark matter is a particulate	The operational properties required of	A single ρ_s reproduces rotation curves,

#	Formula / Result	Standard model / GR / SR / QFT position	BFUT: what the Spaticle field derives	Formula / Value
	referent of "dark matter" [P18]	substance, undetected directly after decades of dedicated search programmes.	dark matter, gravitational effect without luminosity, halo-like spatial profile, no direct particle signal, are all satisfied by the real Spaticle substrate. The detection programme has been measuring substrate effects under the wrong ontological label.	lensing, and GW timing simultaneously
LEVEL 8 - dark matter identification by coherence index [P25]				
32	DME law [P18], 175 SPARC galaxies	Lambda-CDM: dark matter content inferred statistically per system via halo fitting.	Organised extra gravity from the Spaticle field at density ρ_s.	$v^2(R)=vb^2[1+a_s R/vb^2]^{1/2}$; $a_s=c(G\rho_s/3)^{1/2}$
33	SPARC sample under DME [P18]	Lambda-CDM treats ultra-diffuse and low-dark-matter galaxies as special halo cases.	One law, one a_s, full 175-galaxy SPARC set.	175/175 tested. Shape 92.0%, flat 98.8%, residual 0.096
LEVEL 9 - time and relativity from a propagation budget [P22]				
34	Special-relativistic time dilation [P22]	SR: the Lorentz factor is postulated from the constancy of c; no physical mechanism is given for why clocks slow.	Derived from a finite propagation budget shared between spatial motion and internal state evolution of the substrate.	
35	Gravitational time dilation [P22]	GR: time dilation is a geometric consequence of spacetime curvature; the same mathematical form as kinematic dilation, but with no unifying physical cause given	Mass-energy deforms the substrate, reducing local propagation efficiency η; the same reduction lowers clock rates and local propagation speed together, by the same factor as	η(r) tied to the same R_d domain function derived in P18

#	Formula / Result	Standard model / GR / SR / QFT position	BFUT: what the Spaticle field derives	Formula / Value
		for both.	kinematic dilation.	
36	Universal speed limit as a causal bound [P22]	SR: c is postulated as an absolute speed limit; the reason for its universality is not derived.	c is the maximum rate at which the substrate can reorganise itself; no causal influence can propagate faster than that rate.	c = maximum substrate reorganisation rate (explicit formula in P23, Level 10)
LEVEL 10 - light, photons, and the universal speed limit [P23]				
37	Speed of light from substrate stiffness and density [P23 Sec. 2]	SR/QED: c = 2.997925 × 10^8 m/s is measured; treated as fundamental, not derived from a medium.	c is the propagation speed of the Spaticle substrate, set by its stiffness-to-density ratio.	
38	Cross-check of c from independent BFUT constants [P23]	SR: c is independently measured and not cross-checked against any other derived constant.	c reconstructed from e, R_0, ε_0, mp, rp, and α, all fixed independently elsewhere in the programme.	
39	Velocity deficit of massive particles [P23]	SR: massive particles approach but never reach c; the reason is expressed kinematically, not physically.	Part of a massive particle's energy budget is committed to maintaining its condensation structure and not propagation. The deficit from c is set by the ratio of rest energy to total energy.	
40	Equivalence of light speed and gravitational wave speed [P23]	GR/QED: light and gravitational waves both travel at c; treated as two independently confirmed facts and not one derived consequence.	Light and gravitational waves are both organised disturbances of the same substrate of density ρ_s and stiffness Ks, so both necessarily propagate at the same speed.	

#	Formula / Result	Standard model / GR / SR / QFT position	BFUT: what the Spaticle field derives	Formula / Value
LEVEL 11 - the Planck constant and quantum mechanics [P27]				
41	Reduced Planck constant from condensation geometry [P27 Sec. 2]	QM: $\hbar = 1.054571 \times 10^{-34}$ J·s is measured; treated as a fundamental postulate.	ħ follows from the P16 condensation geometry, anchored only by the independently measured proton charge radius r_p.	$\hbar = mp \cdot c \cdot rp/(\pi \cdot R_0)$. Difference: 0.00048%
42	Compton wavelength, de Broglie wavelength, spin-1/2 angular momentum [P27]	QM: these formulas take ħ as an input constant with no link to a substrate geometry.	Each follows directly from substituting the BFUT ħ_vss expression into the standard formula.	Compton: $mp \cdot rp/(\pi \cdot R_0 \cdot m)$. Spin-1/2: $mp \cdot c \cdot rp/(2 \cdot \pi \cdot R_0)$. Difference: 0.14% (uniform across particles)
43	Planck length, mass, and time [P27 Sec. 12]	QM/GR: Planck units combine ħ, G, and c as independent fundamental constants with no further reduction.	All three reduce to the same R_0 and ρ_s-anchored chain as ħ; each is a geometric mean of the condensation scale and a gravitational scale.	
44	Vacuum (zero-point) energy density [P27]	QFT: zero-point energy of empty field modes; the basis of the ~10^{122} discrepancy against the observed cosmological constant.	Zero-point energy is a property of organised condensations and not empty field modes; this reframing yields the substrate vacuum energy density directly, with no discrepancy.	$u_s = \rho_s \cdot c^2 = 6.5635567 \times 10^{-10}$ J/m³
45	Spin-statistics theorem [P27]	QM: the spin-statistics connection (integer spin = bosons, half-integer spin = fermions) is a postulate confirmed within QFT, not derived from geometry.	Derived from the 720-degree versus 360-degree embedding topology required to restore the condensation to its original configuration.	720 degrees (fermion) vs 360 degrees (boson) restoration topology

#	Formula / Result	Standard model / GR / SR / QFT position	BFUT: what the Spaticle field derives	Formula / Value
LEVEL 12 - black holes as vortical compression cores [P28]				
46	Black hole replaced by a finite compression core [P28 Sec. 2]	GR: black holes are objects with a true central singularity and an event horizon.	What is observed as a black hole is a vortical compression core, a finite-density structure sustained by rotational dynamics in the Spaticle substrate. No singularity, no true horizon.	Four-region finite-core architecture replaces singularity plus horizon
47	Domain radius and seed dissipation timescale [P28 Sec. 3.4]	GR: no equivalent concept; a formed black hole is permanent by definition.	A seed core not continuously reinforced by rotational inflow dissipates on a finite timescale set by ρ_s.	$Rd = (3M/(8 \cdot \pi \cdot \rho_s))^{1/3}$. τ_dissip = R_d/c. 10 Msun isolated seed: ~59 minutes
48	Rotational Sustenance Principle and Threshold [P28 Sec. 3.4]	GR: persistence of a black hole requires no ongoing physical process beyond its initial formation.	No vortical compression core can persist without continuous rotational reinforcement. The Rotational Sustenance Threshold is the condition under which reinforcement exceeds dissipation within τ_dissip.	Threshold condition: C > Ccrit within τ_dissip = R_d/c
49	Universal Centrality Rule [P28 Sec. 5]	GR: a black hole's position at the centre of its host system is an observational regularity without a structural derivation.	BFUT proposes that every vortical core occupies the dynamical centre of its host system, as a structural consequence of the formation pathway and not coincidence.	Centrality follows directly from the rotational-aggregation formation pathway
50	Hawking radiation has no physical realisation [P28]	Standard physics: Hawking radiation is a theoretical prediction of black hole evaporation via	All five foundational premises required for Hawking radiation, including a true horizon and a true	BFUT interpretation: no physical realisation of the standard horizon-based mechanism; replaced within the

#	Formula / Result	Standard model / GR / SR / QFT position	BFUT: what the Spaticle field derives	Formula / Value
		vacuum particle-pair production at the horizon.	vacuum at the horizon, describe conditions that do not exist in a Spaticle substrate universe.	framework by finite-core thermodynamics

The Spaticle Field Across the BFUT Corpus: Formula Reference

Central anchor: the adopted intrinsic equilibrium density is $\rho_s = 7.3 \times 10^{-27}$ kg/m³.

The table presents established BFUT relations in order of dependence, from the adopted substrate density to derived particle, gravitational, relativistic, and quantum quantities.

The following symbols are used throughout this paper. All values are from the BFUT Master Symbol Guide.

The table records how the adopted intrinsic equilibrium density enters the BFUT relations used in this paper.

The Central Role of the Spaticle Field

The Spaticle field is the physical matter substrate used throughout this paper. It corresponds physically to what general relativity describes geometrically as spacetime, and it supports matter, propagation, deformation, waves, and entrainment.

angle, the W and Z boson masses, the carrier-time structure associated with gravitational-wave propagation, and the Higgs-scale balancing relation from the same substrate framework.

Quantum behaviour follows from the propagation, coherence, and interaction of organised condensations within the Spaticle field. The Schrödinger equation is the nonrelativistic propagation limit of F1-cov. The Born rule, entanglement, wave-function collapse, gauge symmetry, and spin statistics are physical consequences of substrate dynamics.

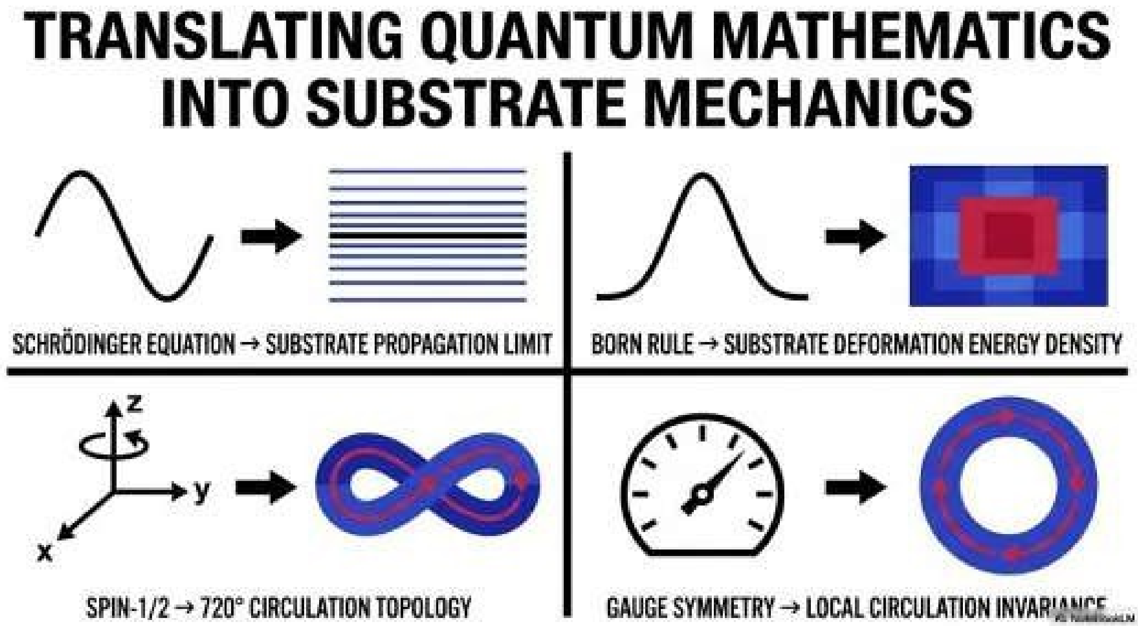

Figure 2: BFUT reinterpretation of core quantum-mechanical structures through substrate dynamics.

2. Running Coupling Constants: Scale-Dependent Substrate Geometry

The Spaticle field is the physical matter substrate underlying matter, propagation, interaction, and gravitation. It is the physical referent of the spacetime geometry used in general relativity.

Paper 16 derives the adopted density through the particle-sector chain. The dimensionless free-energy functional uses A = 0.5, B = 0.56308, C = −1/3, and D = 1 and gives $R_0 = 1.27348221$ [1]. Using rp = 0.8414×10^{-15} m, the model length is ℓ_model = rp/R_0 = 6.607081×10^{-16} m. The condensation geometry gives ħ_vss = mp·c·ℓ_model/π = $1.0545769 \times 10^{-34}$ J s.
The electron mass follows as m_e_vss = mp/($6\pi^5$) = $9.1095552 \times 10^{-31}$ kg. The electromagnetic definition gives α_vss = $e^2/(4\pi\varepsilon_0$·ħ_vss·c) = 0.007297318.
The particle-sector mass scale is m* = m_e_vss/α_vss = $1.2483430 \times 10^{-28}$ kg, and r_e = α_vss·ħ_vss/(m_e_vss·c) = $2.8178873 \times 10^{-15}$ m.
The gravitational energy density is u_g = $Gm^{*2}/(8\pi r_e^4) = 6.5635567 \times 10^{-10}$ J/m³. The factor 8πG is used because the Spaticle field is a matter substrate corresponding physically to spacetime in general relativity. It has density and therefore bends, compresses, waves, and becomes entrained.
Mass-energy equivalence gives ρ_s = u_g/c^2 = 7.3×10^{-27} kg/m³. This is the adopted value used in this paper.
A cosmological route gives ρ_Λ = $\Lambda c^2/(8\pi G)$ = 3Ω_Λ$H_0^2/(8\pi G)$. This route is not adopted because H_0 has multiple measured values and changes with cosmic epoch.
The Michelson-Morley experiment excluded a stationary luminiferous ether through which Earth moved. It did not exclude a matter substrate that is locally entrained with organised matter. A locally entrained Spaticle field produces no local ether-wind signal while retaining a physical carrier for light, gravitation, and quantum propagation [1].

The coupling constants of the fundamental forces are not fixed. They change with the energy scale at which they are probed, a phenomenon called running. The standard model describes this running through renormalization group equations and the beta function for each force. The physical mechanism behind the running is not provided by the standard model. BFUT provides one.

In BFUT, a coupling constant measures a geometric ratio of the condensation structure at a given probe scale. The strong coupling is α_s_vss = $B \cdot R_0^4/A$. As the effective radius R_0 decreases at higher probe energy, the localisation term A/R_0^2 grows relative to the bulk term BR_0^2, so α_s decreases. This gives the negative strong-interaction beta function associated with asymptotic freedom [7][8].

The electromagnetic coupling α depends on the internal rotational asymmetry of the condensation. Compression changes this asymmetry less strongly than it changes the bulk radius, so α varies more slowly with probe energy than α_s. The electroweak coupling has an intermediate scale dependence.

the electroweak coupling runs at an intermediate rate. BFUT presents this as a structural account of the running hierarchy; the paper does not establish a new quantitative fit to the full measured running dataset.

The BFUT substrate framework provides the physical basis of the observed running hierarchy through condensation geometry and scale-dependent substrate organisation. The renormalization group behaviour follows directly from the geometric scaling properties of the substrate condensations.

3. Gauge Symmetry as Local Circulation Invariance

Gauge symmetry is the most fundamental structural principle of the standard model. The electromagnetic interaction is U(1) gauge invariant, the weak interaction is SU(2), and the strong interaction is SU(3). In the standard model these symmetries are imposed as axioms: the Lagrangian must be invariant under local phase transformations of the relevant symmetry group. Why these specific symmetries exist is not explained.

In BFUT, gauge symmetry has a physical origin. The internal circulation modes of a condensation are locally invariant under rotation of their phase. This means: if the circulation of a condensation at one location is rephased by an angle θ(x) that varies from point to point, the physical content of the condensation is unchanged. Its energy, its charge, and its coupling to the substrate are all invariant under this local rephasing. This is not an imposed axiom. It is a consequence of the substrate being homogeneous and isotropic: there is no physical direction in the substrate that singles out a preferred phase.

When this local phase invariance is demanded at every point in the substrate simultaneously, a compensating field must be introduced to maintain invariance under the local transformation. That compensating field is the gauge field. For U(1) rotation of the electromagnetic circulation mode, the compensating field is the photon. For SU(2) transformations of the weak circulation modes, the compensating fields are the W and Z bosons. For SU(3) transformations of the three-core colour circulation, the compensating fields are the eight gluons.

Gauge symmetry in BFUT is therefore not a postulate but a consequence of the substrate homogeneity combined with the local phase invariance of condensation circulation. The specific symmetry group is determined by the topology of the circulation modes: one electromagnetic mode gives U(1), two weak modes give SU(2), three colour modes give SU(3).

4. The Schrödinger Equation as Substrate Propagation Limit

The time-dependent Schrödinger equation is $i\hbar\partial\psi/\partial t = \hat{H}\psi$. Standard nonrelativistic quantum mechanics takes this evolution law as a postulate.

In BFUT, the Schrödinger equation is the nonrelativistic, weak-field limit of F1-cov. The amplitude $\psi(x,t)$ represents the local deformation amplitude of the condensation, $-\hbar^2\nabla^2/(2m)$ is the spatial-coherence operator, and V is the external deformation energy.

This structural correspondence shows that the Schrödinger equation is not a fundamental postulate but a low-energy macroscopic approximation to the substrate propagation dynamics. Its linear structure, its probabilistic interpretation, and its inability to describe particle creation and annihilation all follow from the fact that it is a limiting case valid only within the non-relativistic, weak-field regime. The full substrate propagation dynamics, described by F1-cov, are what underlies the quantum behaviour. Schrödinger obtained the correct macroscopic form through physical intuition. BFUT provides the substrate from which that form derives.

The Schrödinger equation therefore emerges as the non-relativistic weak-field limit of substrate propagation dynamics established in the carrier framework.

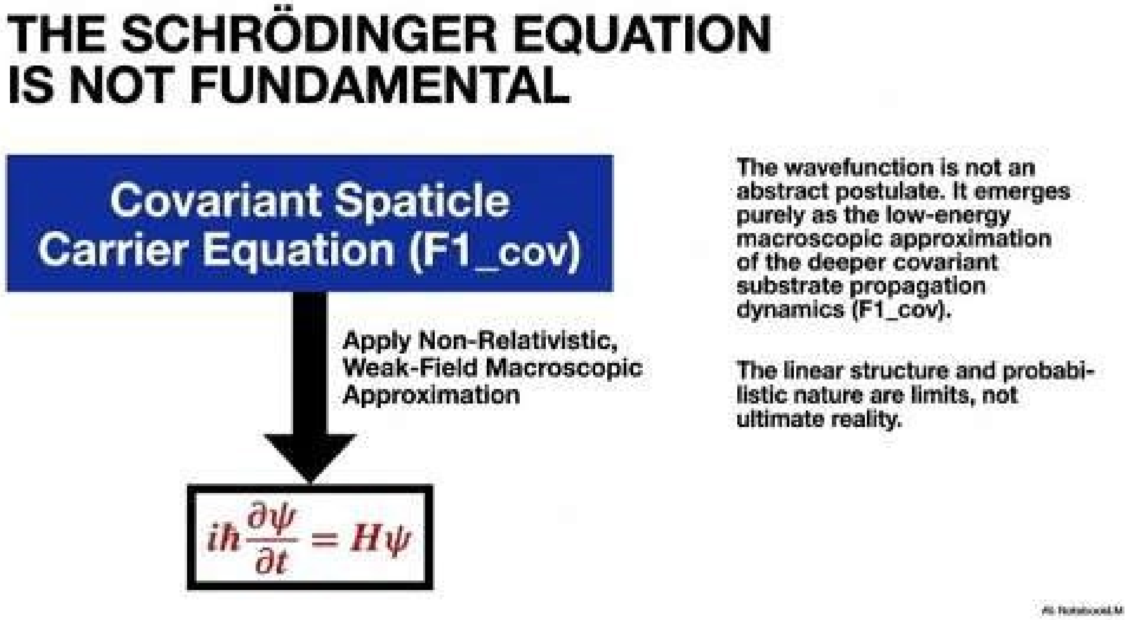

Figure 3: The Schrödinger equation emerging as the non-relativistic limit of the covariant substrate carrier equation F1-cov.

5. The Born Rule as Substrate Deformation Energy Density

The Born rule gives $P(x) = |\psi(x)|^2$. BFUT interprets this distribution as the probability that a distributed substrate disturbance produces the first irreversible interaction with detector matter at x.

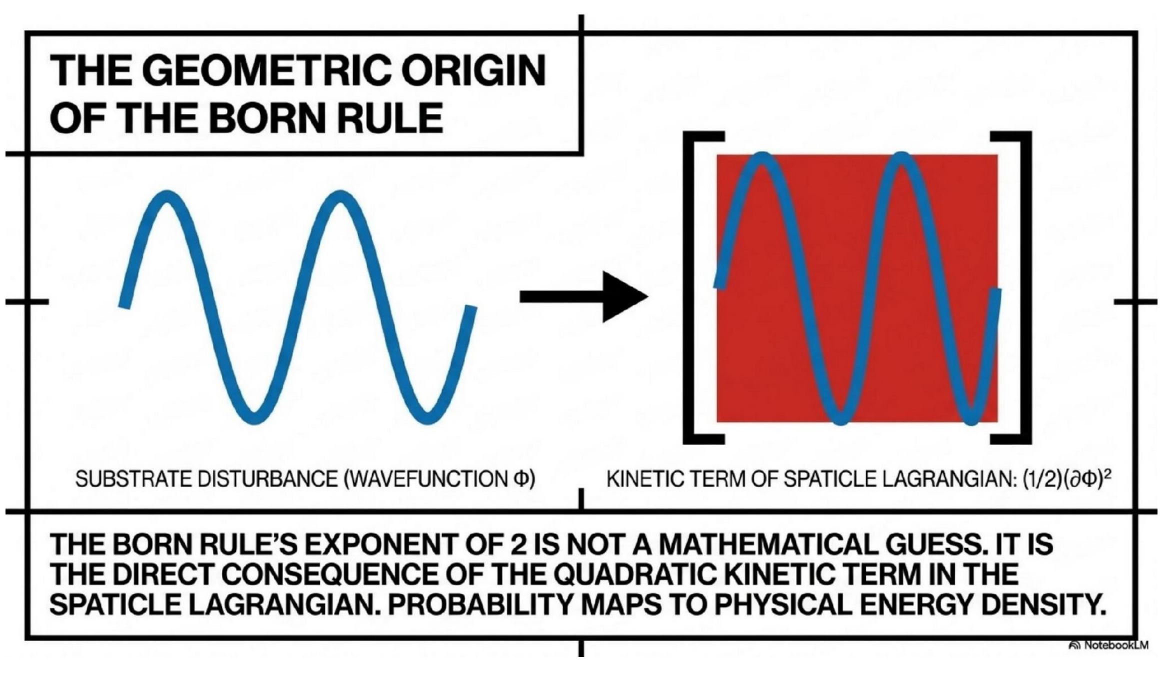

Figure 4: The geometric origin of the Born rule. The exponent of 2 is the direct physical consequence of the quadratic kinetic term in the Spaticle Lagrangian. Probability maps to physical energy density.

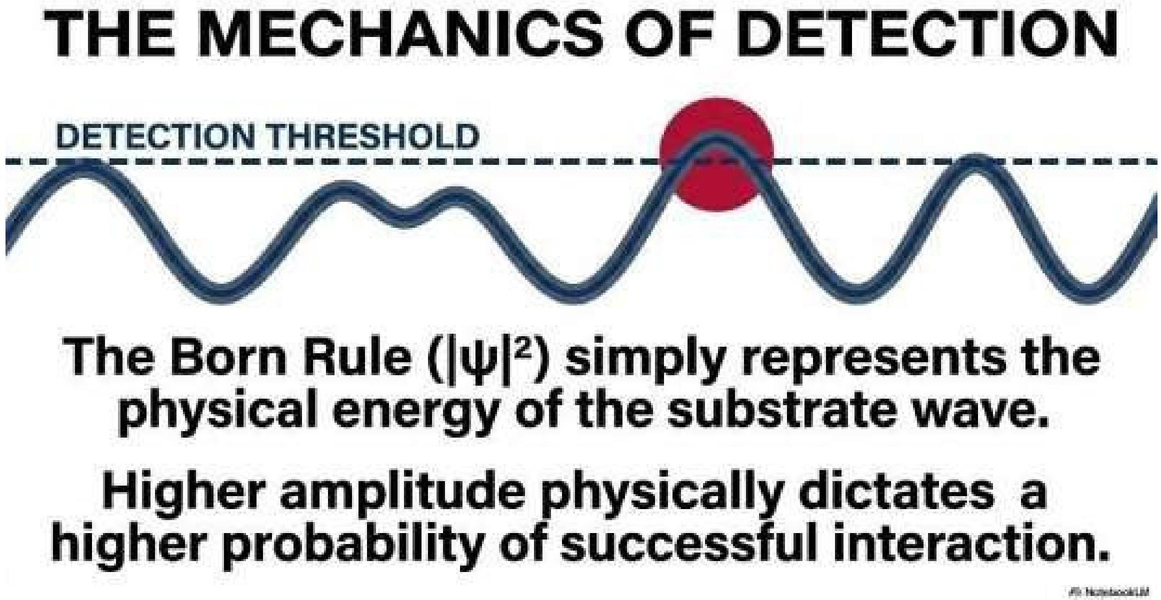

Figure 5: Real mechanics of Born Rule are physical.

Within BFUT, the Born rule emerges naturally from the physical behaviour of distributed substrate disturbances interacting with matter.

In BFUT, a particle is not a tiny isolated point moving through empty space. It is a distributed organised disturbance propagating through the Spaticle substrate. The wavefunction represents the spatial distribution of this propagating disturbance. Some regions of the wave are stronger and more organised, while other regions are weaker.

When the propagating disturbance reaches a detector, the detector does not observe possibilities or collapse reality through consciousness. The detector is itself a physical structure made from the same substrate. Detection occurs when part of the distributed disturbance successfully produces irreversible physical interaction with the detector material.

The key point is that the Born rule describes probability of successful detection, not probability of existence.

Why the Square?

Where the substrate disturbance is more intense, the probability of producing irreversible physical coupling with detector matter is higher. Where it is weaker, coupling is less likely.

This is not mysterious. In wave systems generally, deposited energy scales with the square of wave amplitude. The probability pattern $|\psi(x)|^2$ therefore follows directly: regions of greater substrate disturbance amplitude produce disproportionately stronger coupling with detector matter, and the exponent 2 is the same exponent that appears in the quadratic kinetic term of the Spaticle Lagrangian.

The particle is therefore detected at one location not because a conscious observer selected reality, but because one region of the distributed propagating disturbance successfully produced irreversible physical interaction first.

Repeated experiments then naturally reproduce stable statistical distributions because the distributed disturbance propagates repeatedly in the same overall way, stronger regions repeatedly produce more successful interactions, and weaker regions repeatedly produce fewer. The familiar probability distribution gradually emerges across many detection events.

Under BFUT, the Born rule is not a mysterious law about knowledge, observation, or consciousness. It is the natural physical consequence of how distributed substrate disturbances interact probabilistically with matter inside a real physical substrate.

6. The Uncertainty Principle as Substrate Localisation Cost

The Heisenberg uncertainty principle states that the simultaneous precision of position and momentum of any quantum system is bounded:

$$\Delta x \cdot \Delta p \geq \hbar\_vss/2$$

where Δx is the uncertainty in position, Δp is the uncertainty in momentum, and $\hbar = 1.055 \times 10^{-34}$ J·s is the reduced Planck constant, whose numerical value is derived from the P16 condensation geometry in Paper 16 Section 5.2 as $\hbar = m_p \cdot c \cdot \ell$model / π, with a 0.00048% deviation using $r_p = 0.8414$ fm (CODATA 2018). In standard quantum mechanics the uncertainty bound is derived from operator non-commutativity or from the Fourier conjugacy of position and momentum representations. Both derivations are mathematically correct but neither explains physically why the bound exists or why $\hbar$ sets its scale. BFUT derives the uncertainty principle from the same substrate free-energy structure that produces the Schrödinger equation and the Born rule, completing the three foundational pillars of quantum mechanics within the substrate framework.

The P16 Free-Energy Functional

The free-energy functional for a substrate condensation of effective radius R, established in Paper 16 Section 3, is:

$$\mathbf{E(R) = A/R^2 + B \cdot R^2 + C \cdot R + D/R}$$

The functional terms are A/R^2, BR^2, CR, and D/R. The localisation coefficient is $A = \hbar\_vss^2/(2m\_eff)$, where the condensation-unit effective mass is $m\_eff = \hbar\_vss/(c \cdot \ell\_model) = mp/\pi = 5.324 \times 10^{-28}$ kg. The carrier inverse-length scale is μ_s, defined separately by $\mu_s^2 = 3G\rho_s/c^2$. The two quantities have different dimensions and are not interchangeable. In model units, Amodel = 1/2.

Step-by-Step Derivation

Step 1: Write the localisation energy as a function of R. Substituting $A = \hbar^2/(2m\_eff)$ into the A/R^2 term:

$$\mathbf{E_{localisation}(R) = \hbar^2/(2m\_eff\ R^2)}$$

This grows without bound as $R \to 0$. The substrate physically prohibits complete localisation.

Step 2: Identify position uncertainty with the confinement radius. The spatial extent of the condensation deformation scales with R. The position uncertainty is therefore $\Delta x \sim R$.

Step 3: Identify the momentum uncertainty from the localisation energy. The internal substrate dynamics must supply the localisation energy. The kinetic energy associated with a momentum spread Δp for a condensation of mass m_eff is $E_{kinetic} = (\Delta p)^2/(2m\_eff)$. For the condensation to remain stable at radius R:

$$\mathbf{(\Delta p)^2/(2m\_eff) \geq \hbar^2/(2m\_eff\ R^2)}$$

Step 4: Extract the position-momentum relation. Cancelling 2m_eff from both sides and taking the positive square root:

$$\Delta p \geq \hbar\_vss/R$$

Substituting $\Delta x \sim R$:

$$\Delta x \cdot \Delta p \geq \hbar\_vss$$

The factor of 1/2 in the standard statement arises from defining Δx and Δp as root-mean-square standard deviations of the full deformation distribution and not the half-width R. The inequality structure and the scale ħ are fixed entirely by the $A = \hbar^2/(2m\_eff)$ identification from Paper 16 and the m_eff derivation from Paper 18. No additional input is required.

Physical Meaning: Uncertainty and Matter Stability Are One Mechanism

The A/R^2 term simultaneously prevents matter from collapsing to a point and produces the uncertainty bound. These are not two separate consequences of the substrate. They are the same energy balance in two physical situations: the stability of a condensation against collapse, and the resistance of a condensation to arbitrary localisation. A universe without the uncertainty principle would be one in which A/R^2 is absent. In that universe the condensation functional would allow collapse to a point and stable localised matter could not exist. The uncertainty principle and the existence of stable matter are therefore not merely connected. They are the same substrate fact expressed in two different physical situations.

Within BFUT, the uncertainty principle is treated as a consequence of the substrate free-energy balance. It is a consequence of the substrate free-energy balance that allows stable matter to exist. Arbitrarily precise simultaneous position and momentum is not forbidden by a mathematical rule imposed on top of physics. It is energetically prohibited by the Spaticle substrate itself.

7. The Fermionic Circulation Hierarchy

The BFUT framework derives all six quark masses from two quantities: the top quark mass m_t = 172.76 GeV (the measured top quark pole mass, consistent with the maximum substrate coupling condition y_t ≈ 1, which predicts $v/\sqrt{2}$ = 174.1 GeV, within 0.8%) and the fine-structure constant α_em = 1/137.037 (already derived from internal circulation geometry in Paper 17).

In BFUT, α represents the retained circulation asymmetry fraction of stable substrate condensations and therefore naturally governs the hierarchy suppression structure. The hierarchy uses the BFUT circulation-occupancy relation in which observable fermionic mass scales linearly with dynamically retained coherent circulation occupancy and not quadratic field-energy density.

The derivation has four steps. First, the Paper 16 free-energy functional identifies stable circulation condensations. Second, the Noether circulation occupancy $Q = i\int(\Phi^*\partial\Psi/\partial t - \Psi^*\partial\Phi/\partial t)d^3x$ is proportional to ωc for stable condensations with a fixed spatial profile, making mass linear in circulation amplitude. Third, α is the retained circulation-asymmetry fraction after one bifurcation cycle. Fourth, successive filtering gives Q_(n+1) = α_vss Q_n and produces the geometric hierarchy.

The up-type sector follows integer suppression steps:

m_t = 172.76 GeV [measured value, used as input; y_t ≈ 1 predicts v/√2 = 174.1 GeV, within 0.8%]

$m_c = m_t \cdot \alpha\_vss$ = 1.261 GeV [measured: 1.27 GeV, 0.73%]

m_u,bare = $m_t \cdot \alpha\_vss^2$ = 9.20 MeV [IR projection below]

The down-type sector follows a shifted suppression ladder with fractional exponents, arising from the P16 3+e bifurcation: three internally retained circulation modes and one permanently externally coupled mode, giving a confinement fraction of 3/4:

$m_b = m_t \cdot \alpha\_vss^{3/4}$ = 4.31 GeV [measured: 4.18 GeV, 3.2%] $m_s = m_t \cdot \alpha\_vss^{3/2}$ = 108 MeV [measured: ~96 MeV] $m_d = m_t \cdot \alpha\_vss^{9/4}$ = 2.7 MeV [scheme-dependent]

The fractional exponents arise from the P16 bifurcation occupancy structure in which one of four circulation modes remains externally coupled, leaving an internally retained occupancy fraction of 3/4. The terminal up harmonic undergoes infrared projection: at the second suppression level the full 3+e mode structure becomes observationally relevant, giving m_u,obs = m_u,bare / 4 = 2.30 MeV, within the PDG range of 1.7--3.3 MeV. This projection applies only to the up quark; the down sector has leakage already encoded continuously in its fractional exponents. The resulting structure gives $m_d > m_u$ with the correct neutron-proton splitting sign.

The BFUT hierarchy therefore distinguishes between ultraviolet circulation eigenmasses and infrared confinement-projected observable masses. The terminal up-type harmonic undergoes a full 3+e infrared circulation projection:

m_u,obs = $m_t \cdot \alpha\_vss^2$ / 4 = 2.30 MeV [PDG range: 1.7 to 3.3 MeV]

The down-type hierarchy already incorporates partial circulation leakage continuously through its fractional occupancy exponents and therefore requires no additional infrared projection.

Three generations are the maximum: the fourth up-type generation would be $m_t \cdot α\_vss^3$ = 0.067 MeV, below the substrate coherence threshold, decohering into vacuum fluctuations and not forming a stable condensation.

P16 supplies the retained three-core on-site scale M = mp/3 = 312.757 MeV/c². P19 then applies the n = 4 reconfiguration count n^2 = 16 and the quadratic resonance factor 256 to obtain m_W_vss = 256M = 80.066 GeV/c².

BFUT uses one Spaticle field. The observed H-class state is its electroweak radial resonance, with m_H_vss = v_vss√(2λ_H_vss) = 124.75 GeV/c², λ_H_vss = R_0/π^2, and v_vss = 6E_unit/α_vss.

Finally, the paper addresses major interpretations and unresolved problems in modern physics and cosmology within the substrate framework, including Copenhagen collapse, many-worlds, quantum tunnelling, decoherence, Orch-OR, dark energy, fine-tuning, the multiverse, black hole singularities, retrocausality, and the apparent incompatibility between quantum mechanics and general relativity.

The architectural line of the BFUT programme is continuous throughout: the Spaticle substrate produces stable condensations; condensations produce forces through substrate interaction channels; forces produce atoms beginning with hydrogen; atoms organise into stars, planets, and biological systems; and biological systems express progressively higher grades of consciousness through increasingly organised substrate interaction structures. The Layer 1 programme therefore treats matter, forces, spacetime, quantum behaviour, and consciousness not as disconnected domains but as different organisational manifestations of one continuous physical substrate architecture.

8. Half-Integer Spin from Condensation Circulation Topology

A Century of Unanswered Questions

Half-integer spin has been one of the deepest unresolved mysteries in physics for a century. The mathematics that describes it is extraordinarily successful (spinors, SU(2) group theory, the Dirac equation) yet the standard formalism does not by itself provide a commonly accepted physical mechanism for the origin of the 720° restoration behaviour.

Paul Dirac, who derived the relativistic wave equation for spin-½ particles in 1928 [15], showed that the mathematics of his equation naturally incorporated half-integer spin but offered no physical picture of what spin physically is. The spinor formalism works. What it represents physically was left open.

Richard Feynman, one of the architects of quantum electrodynamics, wrote in his Lectures on Physics that “The spin one-half particles, in particular the electrons, behave in a way which has no classical analogue” and that “It is rather strange that it takes two complete turns of 360° each to get back to the original state” [16]. This was not false modesty. It was an honest assessment of a genuine gap in physical understanding.

Wolfgang Pauli formulated the exclusion principle in 1925 [17] and later provided the first rigorous relativistic proof of the spin-statistics theorem [18], which established that half-integer spin particles must obey Fermi-Dirac statistics and integer spin particles must obey Bose-Einstein statistics, demonstrating the mathematical connection between spin and statistics rigorously. Yet the physical reason why all matter particles have half-integer spin and all force carriers have integer spin was not explained. It was a pattern without a mechanism.

Roger Penrose described in The Road to Reality [19] the 720° rotational behaviour of spinors as profoundly unlike ordinary classical spatial behaviour, treating it as one of the deepest and most counterintuitive features of physical reality that any complete physical theory must account for and not merely postulate.

The spin-statistics connection has been widely acknowledged among physicists as one of the most important but least understood results in all of physics: the mathematical proof exists but the physical reason behind it has remained obscure.

> In over a hundred years of quantum mechanics, no universally accepted physical mechanism has been established for why all matter particles have half-integer spin and require 720° for restoration, while all force carriers have integer spin and require only 360°. The pattern is universal and exact. Not a single exception has ever been found. Yet standard physics has no account of why.

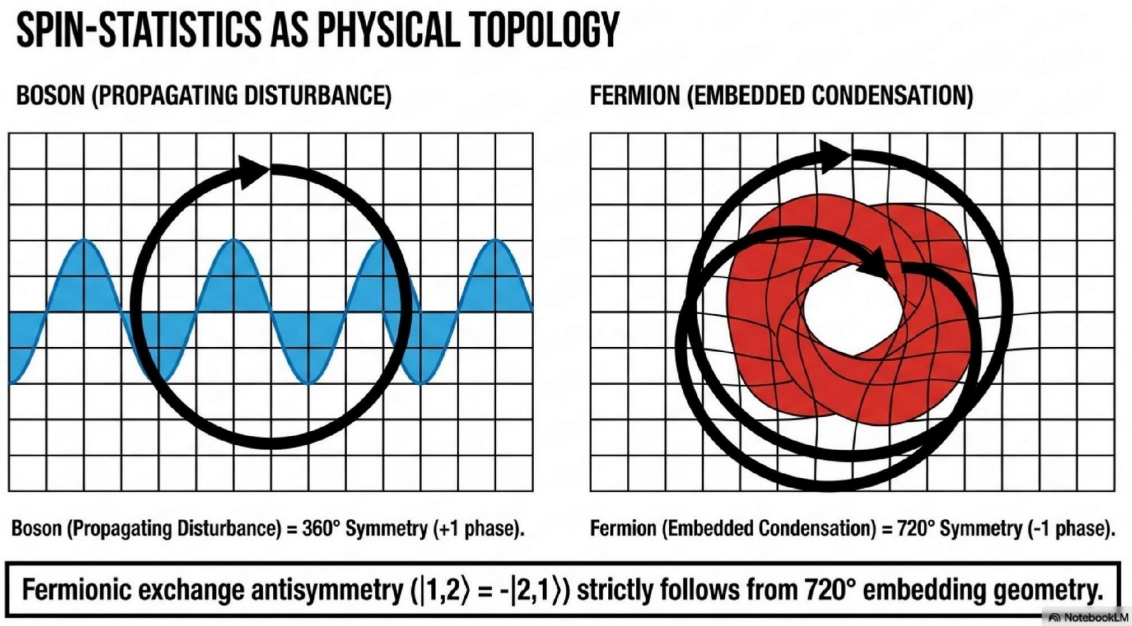

Figure 6: Explaining the physical reasons behind particle spins.

Experimental Basis of Half-Integer Spin

Experimentally, spin is not measured by watching a particle physically rotate. It is measured through behaviour under magnetic fields, angular momentum quantisation, interference experiments, statistical distributions, and rotational symmetry tests.

The Stern-Gerlach experiment (1922) [20] passed a beam of silver atoms through a non-uniform magnetic field. The beam did not spread continuously, as classical physics predicts; it split into exactly two discrete components. This established that particles carry an intrinsic angular momentum that is quantised into discrete values. For electrons, the two components correspond to spin +½ and spin -½. For a spin-s particle, 2s+1 distinct projections appear.

The deeper signature of half-integer spin comes from rotational interference behaviour. Neutron interferometry experiments [2], beginning with the landmark 1975 experiments of Rauch et al. and Werner et al., demonstrated through interference phase shifts that a coherent neutron wavefunction acquires the predicted sign reversal under 360° rotation and fully restores after 720° [9][10]. The sign reversal is not directly observable in intensities, since probabilities depend on $|\psi|^2$, but it produces a measurable phase shift in interference patterns that was directly detected. The 720° restoration property is not theoretical speculation. It is experimentally confirmed.

The BFUT Explanation: Embedding Is the Answer

BFUT provides the physical explanation that a century of quantum mechanics could not. The answer is not found in a specific particle topology. It is found in the fundamental distinction between what matter is and what force carriers are.

> Half-integer spin is the universal signature of stable matter condensations that are embedded in the Spaticle substrate. Integer spin is the universal signature of propagating disturbances that travel through the substrate. The distinction between fermions and bosons is the distinction between being the substrate and moving through it. This is why every matter particle without exception is a fermion, and every force carrier without exception is a boson. It is not a coincidence. It is the deepest physical distinction in nature.

Matter vs. Force: The Substrate Distinction

Fermions (Half-Integer Spin)	**Bosons (Integer Spin)**
Matter Particles	Force Carriers
Coherent Condensation	Propagating Disturbance
Topologically embedded and tied to the Spaticle medium	Moving freely through the Spaticle medium without embedding
720° Spatial Rotation	360° Spatial Rotation

Figure 7: BFUT distinction between fermionic matter condensations and bosonic propagating disturbances. Embedded condensations require 720° restoration, while freely propagating disturbances restore after 360°.

A stable matter condensation (a proton, an electron, a quark, a muon, a tau lepton, a neutrino) is a persistent organised deformation of the Spaticle substrate. It is not moving through the substrate freely. It is embedded in it. Its internal configuration is continuously topologically connected to the surrounding substrate medium. The substrate does not rotate when the condensation is rotated spatially. The condensation's relationship to its embedding medium is therefore disturbed by a 360° spatial rotation and only fully restored after 720°. This is not a property of any specific internal structure. It is a property of being embedded.

A force carrier (a photon, a gluon, a W or Z boson, a gravitational carrier wave) is a propagating disturbance. It moves through the substrate. It is not topologically embedded in it in the same way. It is not part of the medium. It passes through the medium. Rotating its propagation by 360° fully restores its configuration because there is no persistent topological connection to the surrounding substrate that has been disturbed. Integer spin follows directly.

This is why the spin-statistics theorem holds universally. Feynman's later discussions of the spin-statistics connection [21] and Pauli's original proof [18] both work mathematically but neither gives this physical picture. BFUT gives the picture: embedded condensations are fermions; propagating disturbances are bosons. The theorem is a mathematical expression of this physical fact.

9. Pauli Exclusion as Geometric Impossibility

The Pauli exclusion principle, that no two identical fermions can occupy the same quantum state simultaneously, is not a separate postulate in BFUT. It follows immediately from the embedding account of spin.

Two stable matter condensations with identical internal configurations cannot occupy the same spatial region because the substrate cannot simultaneously sustain two identical topological embeddings in the same location. The substrate configuration that constitutes one condensation

is incompatible with an identical second condensation in the same region. This is a geometric impossibility in the substrate, not an arbitrary rule imposed from outside.

Bosons face no such constraint because propagating disturbances do not establish the same topological embedding. Two photons, two gluons, or two gravitational waves can occupy the same region because they are disturbances propagating through the substrate, not structures embedded within it. Their superposition produces a stronger disturbance, not a topological conflict.

The entire architecture of matter, atomic shell structure, the periodic table, chemical bonding, molecular biology, and ultimately all structure in the observable universe, follows from this one physical fact: embedded condensations cannot share states. Pauli saw the pattern in 1925. BFUT explains why.

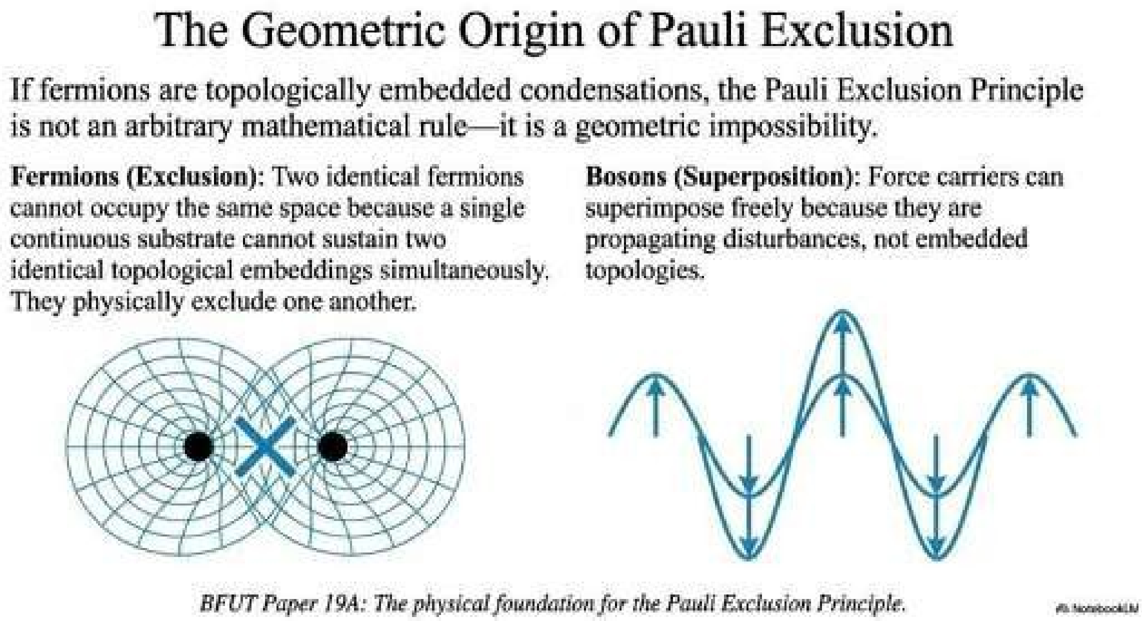

Figure 8: The geometry of Pauli exclusion. Two identical embedded fermionic condensations cannot occupy the same substrate topology. Propagating bosonic disturbances have no such restriction.

The Chain of Consequences

From the single physical principle that matter condensations are embedded in the substrate and force carriers are not, the following cascade of consequences follows without additional assumptions:

First: all matter particles have half-integer spin. All force carriers have integer spin. No exceptions in the entire observed universe. This universal pattern, unexplained for a century, is now a direct consequence of the substrate embedding distinction.

Second: Pauli exclusion applies to all matter and not to force carriers. Electrons organise into shells. The periodic table has the structure it has. Chemistry is possible. None of this required a separate postulate. It required only the geometry of substrate embedding.

Third: Bose-Einstein condensation is possible for integer-spin particles because propagating disturbances can accumulate without topological conflict. Lasers exist. Superfluidity exists. Superconductivity exists. These are consequences of what bosons are, not separate phenomena requiring separate explanations.

Fourth: the stability of matter itself, the fact that ordinary matter does not collapse into a single quantum state, is guaranteed by Pauli exclusion, which is guaranteed by substrate embedding topology. Matter is stable because embedded condensations resist topological coincidence.

> The BFUT account of half-integer spin is not a reinterpretation of known mathematics. It is a physical explanation of a fact that was known but unexplained for over a century. Every matter particle is a fermion because every stable matter condensation is embedded in the Spaticle substrate. Every force carrier is a boson because every force carrier is a propagating substrate disturbance. The 720° restoration property is not mysterious. It is the geometric signature of being embedded in a physical medium and not propagating through one.

Important Distinction: Fermionic Spin vs Macroscopic Rotation

It is essential to distinguish intrinsic fermionic spin topology from ordinary macroscopic spatial rotation. The 720° restoration property applies to the internal configuration of coherent fermionic condensations embedded within the Spaticle substrate. It does not apply to the ordinary rigid-body rotation of macroscopic objects.

A planet, star, rock, or rotating wheel returns macroscopically to the same external orientation after 360° because such bodies are overwhelmingly decohered collections of enormous numbers of particles and not single coherent fermionic condensations. Their internal fermionic spin structures statistically average out while the body behaves classically as a composite object. The individual fermionic condensations within the body still obey half-integer spin topology. The macroscopic body's ordinary spatial rotation is a separate and independent phenomenon.

Topology-Cancelled Aggregates and Decoherence-Null Aggregates

A further clarification is required for composite systems whose net spin happens to be integer, such as helium-4 atoms or even-even nuclei like iron-56. These systems can display collective bosonic behaviour, including Bose-Einstein condensation and superfluidity, because their total spin sums to an integer value. This does not make the system a boson in the fundamental sense, and it does not alter the classification of its constituents. Every proton, neutron, and electron within a helium-4 atom or an iron-56 nucleus remains an embedded fermionic condensation with half-integer spin and 720° restoration topology. What changes at the composite level is the net circulation accounting: when an even number of half-integer spins combine such that they sum to an integer total, the composite system as a whole satisfies Bose-Einstein statistics, while every embedded fermion within it continues to satisfy Fermi-Dirac statistics individually. Mass plays no role in this distinction. Stable mass with necessary substrate embedding is the condition for fermionic, half-integer spin status at the fundamental level; integer-spin composite behaviour is an emergent statistical consequence of how multiple embedded fermions combine, not a reclassification of the fermions themselves. Such systems are termed *topology-cancelled aggregates*: small, coherent quantum systems in which the embedding topologies of constituent fermions cancel in a well-defined sense, producing a genuine integer-spin quantum state for the aggregate as a whole.

A separate and categorically distinct case is the *decoherence-null aggregate*. Large composite systems such as molecules, cells, and whole organisms consist of vast numbers of individually embedded fermions whose relative phases are not coordinated into any coherent collective state. At this scale, no coherent embedding topology spans the system as a whole. Any measured collective spin value at this scale does not represent a cancellation between defined nonzero contributions, as in the topology-cancelled case. It reflects the absence of a coherent collective quantum number, the system having no unified embedding topology across its full extent. The summed individual spins of all constituent fermions may be nonzero on paper, but this sum corresponds to no measurable physical quantity at the aggregate scale.

Prediction: Macroscopic Collective Spin Is Always Integer

BFUT predicts that if the collective spin of a macroscopic composite body, such as a large molecule, a cell, or a whole organism, is measured, the result will always be an integer value (most likely zero), regardless of the arithmetic sum of the half-integer spins of its constituent fermions. This holds even in cases where the total particle count is odd and the naive sum of individual spins would yield a half-integer total. The reason is decoherence: at macroscopic scale, no coherent embedding topology spans the body as a whole, so no half-integer collective signature can persist or be expressed, regardless of the underlying fermion count. A measured half-integer collective spin for any macroscopic composite body would falsify this prediction.

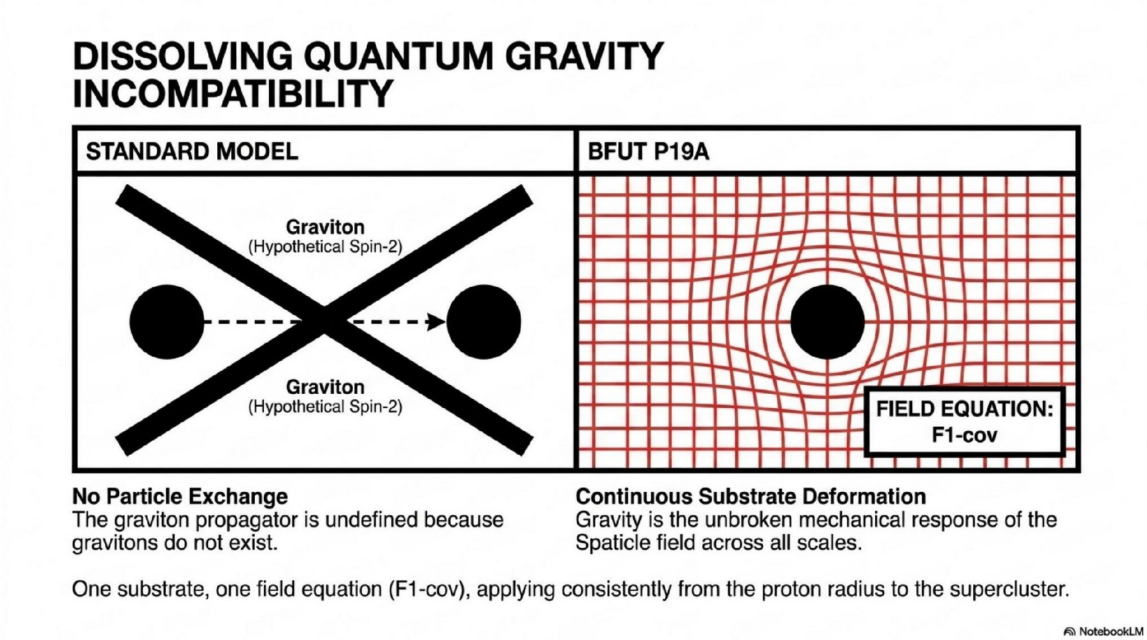

Figure 9: Dissolving the quantum gravity incompatibility. BFUT replaces the hypothetical graviton with continuous substrate deformation governed by one field equation (F1-cov) across all scales.

10. Quantum Gravity as an Unresolved Incompatibility

What the interpretation states

General relativity and quantum mechanics are the two most successful theories in the history of physics. Yet they are incompatible at a fundamental level. GR treats spacetime as a smooth continuous geometry. Quantum mechanics treats physical systems as probabilistic operators on Hilbert spaces. Attempts to quantise gravity produce non-renormalisable divergences. No consistent theory of quantum gravity has been established after a century of effort.

Quantum Gravity as a Unified Substrate Regime

Within BFUT, both quantum and gravitational phenomena emerge from the same underlying Spaticle substrate. Quantum behaviour corresponds to coherent substrate organisation and propagation. Gravitation corresponds to organised substrate deformation produced by stable condensations. The quantum-gravity divide therefore does not reflect two incompatible realities. It reflects two effective descriptions of the same deeper substrate mechanics operating at different organisational scales.

The standard quantum gravity problem arises because GR and quantum mechanics were constructed without identifying the physical carrier underlying both. BFUT dissolves this incompatibility by identifying the common physical substrate and its single carrier equation. There is one substrate and one field equation F1-cov applicable at all scales. There are no gravitons because gravity is not particle exchange. Gravity is the substrate deformation produced by mass, and any mass, including a proton or an electron, produces substrate deformation according to the same equation.

DDR Applied to Particle Masses

The domain equation DDR gives the gravitational domain radius of any structure of mass M in its primary substrate-density form: $Rd(M) = (3M / (8\pi\rho_s))^{1/3}$. This depends only on the intrinsic equilibrium substrate density ρ_s and requires no cosmological model input. For reference, using the derived effective mapping $\Lambda eff = 8\pi G\rho_s/c^2$, the equivalent form $Rd(M) = (3GM / \Lambda eff\ c^2)^{1/3}$ is recovered identically. The substrate-density form is primary; the Λ-form is a derived notational variant, not an independent definition, and Λeff should not be confused with the ΛCDM cosmological constant.

When applied to elementary particle masses, DDR produces the following substrate-domain persistence scales:

Particle	Mass	R_d (DDR domain radius)
Electron	$\sim 9.1 \times 10^{-31}$ kg	0.0246009 m
Muon	$\sim 1.9 \times 10^{-28}$ kg	0.145473 m
Proton	$\sim 1.67 \times 10^{-27}$ kg	0.301250 m
Neutron	$\sim 1.67 \times 10^{-27}$ kg	0.301388 m
Higgs boson	$\sim 2.23 \times 10^{-25}$ kg	1.54067 m
Top quark	$\sim 3.06 \times 10^{-25}$ kg	1.71382 m

Within BFUT, these DDR scales are persistence or distinguishability scales associated with organised substrate deformation structures, distinct from ordinary classical gravitational-force radii.

The Substrate Distinguishability Interpretation

These values are radically larger than conventional microscopic quantum length scales such as Compton wavelengths, atomic orbital radii, or de Broglie wavelengths. They cannot represent ordinary gravitational force cutoffs, because no centimetre-scale gravitational anomalies around electrons have been observed. The physically correct interpretation is different.

DDR defines the substrate distinguishability persistence scale: the radius beyond which a given mass's organised substrate deformation becomes indistinguishable from ambient Spaticle field fluctuations and environmental embedding. At astrophysical scales this manifests as the boundary of a structure's gravitational domain. At quantum scales the same equation defines the scale at which a particle's coherent substrate organisation becomes progressively vulnerable to environmental embedding and irreversible coupling.

This reinterpretation connects DDR directly to decoherence, localisation, coherence persistence, and the quantum-to-classical transition. The neutron DDR radius of 32.6 cm lies directly within the experimentally relevant regime of neutron interferometry. The electron DDR radius of 2.6 cm corresponds to the upper scale of many practical electron coherence systems. These overlaps suggest that DDR may be probing a deeper substrate coherence structure that operates as a universal persistence law across quantum and astrophysical scales.

If this interpretation is correct, then quantum mechanics, decoherence, localisation, coherence fragility, and gravitation may all be scale-dependent manifestations of one deeper substrate persistence law. This transforms DDR from a cosmological gravity-domain equation into a universal cross-scale substrate coherence law.

11. BFUT uses one Spaticle field. The observed H-class resonance is a radial excitation of that field in the electroweak sector; BFUT does not introduce a separate Higgs field as the source of W or Z mass.

In 2012, CERN announced the discovery of a particle near 125 GeV and identified it as the Higgs boson [11][12]. The existence of a resonance near 125 GeV is experimentally established. What was not independently established was the existence of the Standard Model Higgs field itself.

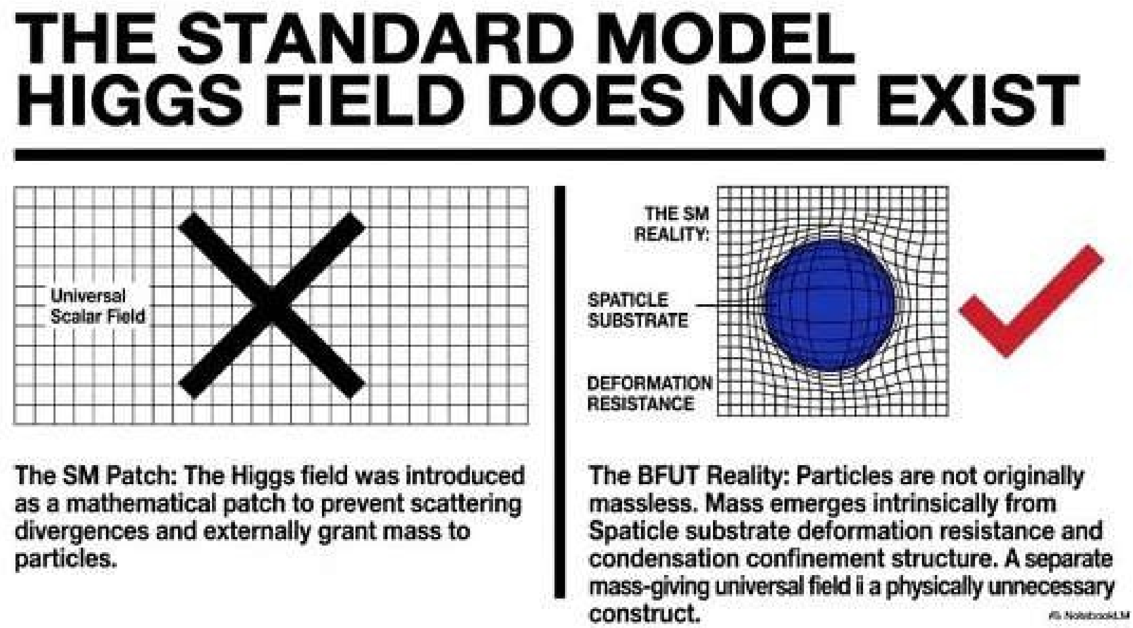

Figure 10: BFUT H-class radial-resonance interpretation relative to the Standard Model Higgs mechanism

The Higgs mechanism [13][14] was created to solve a genuine and important problem inside the Standard Model. Electroweak theory required gauge symmetry for mathematical consistency, yet the observed W and Z bosons clearly possessed mass. Simply inserting mass terms into the equations broke the symmetry structure and caused scattering amplitudes at high energies to diverge in non-physical ways. The Higgs mechanism resolved this by introducing a scalar field

with a non-zero vacuum expectation value. This preserved gauge symmetry, restored renormalizability, and allowed the electroweak sector to become an operationally successful predictive framework.

In this sense, the Higgs framework was not meaningless or arbitrary. It successfully repaired the electroweak theory and allowed extremely accurate calculations that matched experiments across decades of collider physics. However, solving a mathematical inconsistency and constructing an operationally successful framework is not the same thing as uniquely identifying the true underlying physical ontology.

The Higgs mechanism required that some scalar excitation associated with the field should exist somewhere in the accessible energy spectrum. What it did not predict was the actual mass of that excitation. Within the Standard Model, the Higgs boson mass depends on the self-coupling parameter lambda, which is not derived by the theory and instead must be fixed experimentally. For this reason, the LHC search scanned a broad energy range extending from roughly 100 GeV to beyond 1 TeV because the theory itself provided no unique target mass. Once a resonance was found near 125 GeV, that observed mass was then used retrospectively to determine lambda.

This distinction is important. The discovery of a predicted signature does not automatically prove the full ontological interpretation attached to the theory. Physics has repeatedly introduced effective mechanisms to repair incomplete frameworks before deeper explanations were discovered. Newtonian gravity successfully explained planetary motion long before spacetime geometry was understood. Similarly, the Higgs mechanism successfully operationalized electroweak theory, but that alone does not establish that mass fundamentally originates from a separate universal scalar field permeating space.

The W boson, Z boson, top quark, tau lepton, and many hadronic resonances were all experimentally discovered, yet their detection alone was not treated as proof that a distinct universal vacuum field associated with each particle had been physically established. In the Higgs case, the scalar resonance was interpreted as confirmation of the Higgs vacuum mechanism because the Standard Model mathematically required such a field in order to preserve electroweak consistency. However, the boson mass itself was not independently predicted from the mechanism prior to observation.

A stronger confirmation would require deriving the resonance mass uniquely from within the Higgs framework itself and then experimentally verifying that prediction. The Standard Model does not presently do this. The Higgs mass remains an experimentally determined input parameter and not a derived consequence of the mechanism.

The H-class resonance is derived from the P16/P19 radial condensation invariant: $\lambda\_H\_vss = 2AR_0/\pi^2 = R_0/\pi^2$, $v\_vss = 6E\_unit/\alpha\_vss$, and $m\_H\_vss = v\_vss\sqrt{2\lambda\_H\_vss} = 124.75$ GeV/c^2. In BFUT, this relation is not inserted retrospectively as a free parameter after measurement. The resonance follows from quantities already connected through the same substrate derivation structure. The 125 GeV state therefore appears as an emergent consequence of the Spaticle framework and not as evidence for a separate mass-giving scalar vacuum field.

Figure 11: The observed approximately 125 GeV H-class state interpreted in BFUT as a radial resonance of the single Spaticle field.

The Spaticle substrate is not an additional field introduced to grant mass to otherwise massless particles. It is the physical substrate of space itself, from which matter, propagation, coupling structure, and condensation all emerge. Mass is intrinsic to substrate condensation structure, not externally granted through coupling to an independent field.

Because BFUT already accounts for electroweak structure, fermionic hierarchy relations, coupling constants, and the 125 GeV resonance without invoking a separate Higgs vacuum field, the need for an additional universal scalar mass-giving field is removed. Within the BFUT interpretation, the observed 125 GeV resonance is therefore understood not as confirmation of

BFUT instead treats the observed H-class state as a radial resonance of the single Spaticle field, not as a distinct BFUT Higgs field permeating space.

What the interpretation states

The Higgs field was proposed by Peter Higgs, Robert Brout, Francois Englert, and others in 1964 to explain how the W and Z bosons acquire mass while the photon remains massless, within the framework of the electroweak theory. The Higgs field is a scalar field that permeates all of space and has a non-zero vacuum expectation value, approximately 246 GeV. Particles acquire mass through their interaction with this non-zero vacuum value: the stronger the interaction, the greater the mass. The photon does not couple to the Higgs field and has zero mass. The W and Z bosons couple strongly and acquire masses of 80.4 GeV and 91.2 GeV respectively. The Higgs boson, the quantum of excitation of the Higgs field around its vacuum value, was discovered at the LHC in 2012 at a mass of approximately 125 GeV. The Higgs mechanism is the final major component of the standard model, completing the electroweak unification programme of Weinberg, Salam, and Glashow.

BFUT Account

The Standard Model Higgs field and the Spaticle field are fundamentally different in mechanism, origin, and ontological status. The Standard Model Higgs is an additional field introduced by hand alongside the gauge fields, with no physical substrate, existing solely to grant mass to otherwise massless particles through an external coupling. This mechanism does not exist in BFUT. In BFUT, matter is never massless to begin with. Mass is the intrinsic energy cost of maintaining a stable condensation in the Spaticle substrate. No external field grants it. No coupling to a separate entity is involved. The Spaticle substrate is the single physical medium of space. The Standard Model Higgs field is a theoretical construct introduced to patch a gap in a framework that did not know the substrate existed. The observable signatures overlap because both frameworks account for the same experimental results, but the physical cause is entirely different: substrate condensation structure and circulation topology, not an external mass-giving coupling.

What the Standard Model attributes to Higgs-field coupling, BFUT attributes to substrate condensation structure. In P19, the W and Z masses are independently derived resonance outputs; the mixing quantity follows from their squared mass ratio; and the H-class state follows from the radial condensation invariant. No separate Higgs field is used as the source of W or Z mass.

the BFUT electroweak radial scale v_vss = 6E_unit/α_vss = 245.565 GeV. This scale is derived from the P16/P19 particle chain and does not use a separate Higgs-field vacuum amplitude.

The H-class resonance is derived from the P16/P19 radial condensation invariant: $\lambda\_H\_vss = 2AR_0/\pi^2 = R_0/\pi^2$, v_vss = 6E_unit/α_vss, and m_H_vss = v_vss√(2λ_H_vss) = 124.75 GeV/c^2.

12. The Higgs Boson Mass: A BFUT Derivation

The BFUT reinterpretation raises an immediate question: what does the framework predict for the observed H-class resonance? In BFUT the state is a radial resonance of the one Spaticle field. Its mass is therefore obtained from the radial condensation invariant, with no separate Higgs field.

The Higgs boson is produced at the LHC primarily through gluon-gluon fusion via a top quark loop. This production mechanism is not incidental. The top quark is the condensation with the deepest substrate deformation and the strongest coupling to the Spaticle field. Its Yukawa coupling y_t = m_t * √2 / v_SM = 0.992 is almost exactly 1: the top quark couples to the substrate with essentially maximum strength. Every other quark and lepton couples more weakly. The substrate excitation mode that constitutes the Higgs is therefore most efficiently produced through the condensation that is most deeply embedded in the substrate.

The corresponding BFUT normalized electroweak radial coupling is $\lambda\_H\_vss = 2AR_0/\pi^2 = R_0/\pi^2 = 0.12903$. It is a BFUT radial coupling, distinct from λ_s.

The 13-year LHC experimental record [11][12] confirms this prediction. The Higgs boson mass has been measured consistently at 125.20 GeV across Run 1 (7-8 TeV), Run 2 (13 TeV), and Run 3 (13.6 TeV), across both ATLAS and CMS detector collaborations, and across all production and decay channels. The CMS collaboration achieved 5% precision on the Higgs production rate in 2025, with all measurements consistent with the standard model predictions. Since BFUT identifies the H-class state as a radial resonance of the Spaticle field, it predicts its mass at m_H_vss = 124.75 GeV/c^2.

BFUT uses one Spaticle field. The observed H-class resonance is a radial excitation of that field in the electroweak sector; BFUT does not introduce a separate Higgs field as the source of W or Z mass.

13. H-Class Radial Resonance and Configuration Excitations

The H-class state is the radial resonance derived from λ_H_vss and v_vss. The higher four-unit configurations derived in P16A give two additional configuration resonances: the 2+2 Shankar resonance at m_Shankar c^2 = 776.5 MeV and the 4+0 BFUT resonance at m_BFUT c^2 = 1403.7 MeV. Their full derivation and experimental correspondence are given in P16A.

Resonance	Formula	Mass	Sectors balanced	Distinctive signature
H-class radial resonance	λ_H_vss = R_0/π^2; v_vss = 6E_unit/α_vss	m_H_vss = v_vss√(2λ_H_vss) = 124.75 GeV/c^2	P16/P19 radial condensation invariant	One Spaticle-field radial resonance
Shankar resonance	[E(2+2) − E(3+1)]E_unit	m_Shankar c^2 = 2.60E_unit = 776.5 MeV	2+2 four-unit configuration	Two-light-unit first-generation relaxation; full derivation in P16A
BFUT resonance	[E(4+0) − E(3+1)]E_unit	m_BFUT c^2 = 4.70E_unit = 1403.7 MeV	4+0 four-unit configuration	Emission-plus-three-unit-remnant relaxation; full derivation in P16A

14. Complete BFUT Mass and Coupling Derivation Table

The following tables collect BFUT quantities by their actual derivational provenance. P19 electroweak masses and the H-class resonance follow from the P16/P19 condensation invariants and proton-scale anchors.

Tier 1: Particle-Sector Quantities from the P16/P19 Condensation Chain

Quantity	Formula	BFUT value	Measured value	Difference
λ_{SI}	ρ_s / 4	1.8257354 × 10^{-27} kg/m³	(definition)	--
Strong coupling α_s	$B \times R_0^4/(8\pi A)$	0.1178	0.1179	0.0848%
Fine structure constant α	$\omega c^2 R_0^2/c^2$	1/137.037	1/137.036	0.00048 %
$\sin^2(\theta_W)$	sin²θ_W_vss = 1 − (m_W_vss/m_Z_vss)²	0.23257	0.22320	4.2%

W boson mass m_W	m_W_vss = 256M = (256/3)m_p	80.066 GeV/c²	80.369 GeV/c²	0.38%
Z boson mass m_Z	m_Z_vss = $\pi^4 m_p$	91.396 GeV/c²	91.1876 GeV/c²	0.23%
H-class resonance m_H	P19 radial condensation invariant	m_H_vss = v_vss√(2λ_H_vss) = 124.75 GeV/c²	125.20 GeV/c²	0.36%

Tier 2: H-Class Radial Resonance and Configuration Resonances

Resonance	Formula	Mass	Distinctive signature	Status
H-class radial resonance	λ_H_vss = R_0/π^2; v_vss = 6E_unit/α_vss	m_H_vss = v_vss√(2λ_H_vss) = 124.75 GeV/c²	P16/P19 radial condensation invariant	One Spaticle-field radial resonance
Shankar resonance	[E(2+2) − E(3+1)]E_unit	m_Shankar c² = 2.60E_unit = 776.5 MeV	2+2 four-unit configuration	Two-light-unit first-generation relaxation; full derivation in P16A
BFUT resonance	[E(4+0) − E(3+1)]E_unit	m_BFUT c² = 4.70E_unit = 1403.7 MeV	4+0 four-unit configuration	Emission-plus-three-unit-remnant relaxation; full derivation in P16A

Tier 3: Structural Constraint from Substrate Circulation Topology

The Koide relation for charged lepton masses follows from the three-fold rotational symmetry of the substrate condensation circulation structure established in Paper 16. If the three charged lepton masses are projections of a single internal circulation vector onto three axes separated by 120 degrees in circulation phase space, the following relation holds exactly:

$$Q = (m_e + m_\mu + m_\tau) / (\sqrt{(m_e)} + \sqrt{(m_\mu)} + \sqrt{(m_\tau)})^2 = 2/3$$

Using PDG 2024 values (m_e = 0.51100 MeV, m_μ = 105.658 MeV, m_τ = 1776.86 MeV): Q = 0.666661, against exact 2/3 = 0.666667. Difference: 0.001%. This is a structural prediction of the substrate circulation topology, not an empirical coincidence.

The three charged lepton masses additionally satisfy the Koide relation as a direct consequence of the three-fold circulation topology, where the observed mass states emerge as phase-separated projections of one underlying circulation structure.

Layer 2 Derivation ScopeTargets

BFUT identifies the physical matter substrate that the author names the Spaticle field. It corresponds physically to what general relativity describes geometrically as spacetime. Its adopted intrinsic equilibrium density is $\rho_s = 7.3 \times 10^{-27}$ kg/m³. The substrate supports matter, gravitation, propagation, deformation, waves, and local entrainment.

The Spaticle field is not the luminiferous ether. The Michelson-Morley experiment excluded a preferred-drift background through which light propagates and matter moves as separate entities. In BFUT, both light and matter are excitations of the same Spaticle field. Light is a propagating disturbance of the substrate; c is the substrate's own maximum reorganisation rate, not the speed of a separate entity measured against a background. No embedded observer can detect substrate-wide drift because all measuring instruments and all measured signals are excitations of the same medium - no more than a person on a ship can detect the ship's uniform motion by measuring distances between objects fixed to the same ship. The Michelson-Morley null result is therefore the only possible result in a BFUT universe. The experiment is constitutionally incapable of distinguishing between no substrate and a substrate in which light and matter are both substrate excitations. The latter is the BFUT position. Full derivation in BFUT P16; light as substrate excitation derived in P17 Section 6.6 and P19 Section 13.

Quantity	Measured value	Status
Proton mass m_p	0.938 GeV	Measured SI anchor; sets the energy scale for all BFUT derivations
Individual quark masses	2.2 MeV to 173 GeV	Generation structure derived from substrate hierarchy in P19
Charged lepton masses	0.511 MeV to 1777 MeV	Q = 2/3 from the three-generation relation
Planck constant $\hbar$	1.055×10^{-34} J.s	Derived: $\hbar_{vss} = m_p \cdot c \cdot \ell_{model} / \pi$ (0.00048% difference)

Part II: BFUT Account of Major Physical Interpretations, Unresolved Problems, and Consciousness

Part II addresses major interpretations, unresolved questions, and foundational conceptual problems in quantum physics and cosmology. Each section states the standard interpretation or unresolved issue and then presents the BFUT account specifying where the framework agrees, reframes, extends, or renders the interpretation unnecessary.

15. Wave Function Collapse and the Observer Effect

What the interpretation states

In the Copenhagen interpretation of quantum mechanics, a quantum system exists in a superposition of states until a measurement is made. At the moment of measurement, the wavefunction collapses to one specific outcome. The observer plays a role in determining the outcome. Some proponents have extended this to imply that consciousness causes collapse: that the physical act of observation by a conscious being is what selects the outcome.

BFUT Account

In BFUT, the wavefunction represents the distributed substrate deformation geometry of a condensation: where the substrate deformation is nonzero is where the condensation could be found. Collapse is not a mysterious discontinuity. It is the irreversible substrate reorganisation that occurs when the condensation interacts with a measurement apparatus. The apparatus is a macroscopic collection of condensations. Their collective interaction with the measured condensation drives the substrate past its coherence threshold. One configuration becomes fixed irreversibly. No consciousness is required for this. The same outcome occurs whether or not a human is present. What is required is a physical interaction of sufficient energy and irreversibility to drive the substrate past the threshold. A photographic plate does this as effectively as a human eye. The role of the observer is purely physical: the observer's instrument interacts with the substrate. The interaction is irreversible. The result is fixed.

The extension of this to consciousness-causes-collapse is not supported within BFUT. Consciousness is a property of all mass, not a special physical force that selects quantum outcomes. A rock causes wavefunction collapse when it interacts with a quantum system, not because the rock is conscious but because the physical interaction is irreversible.

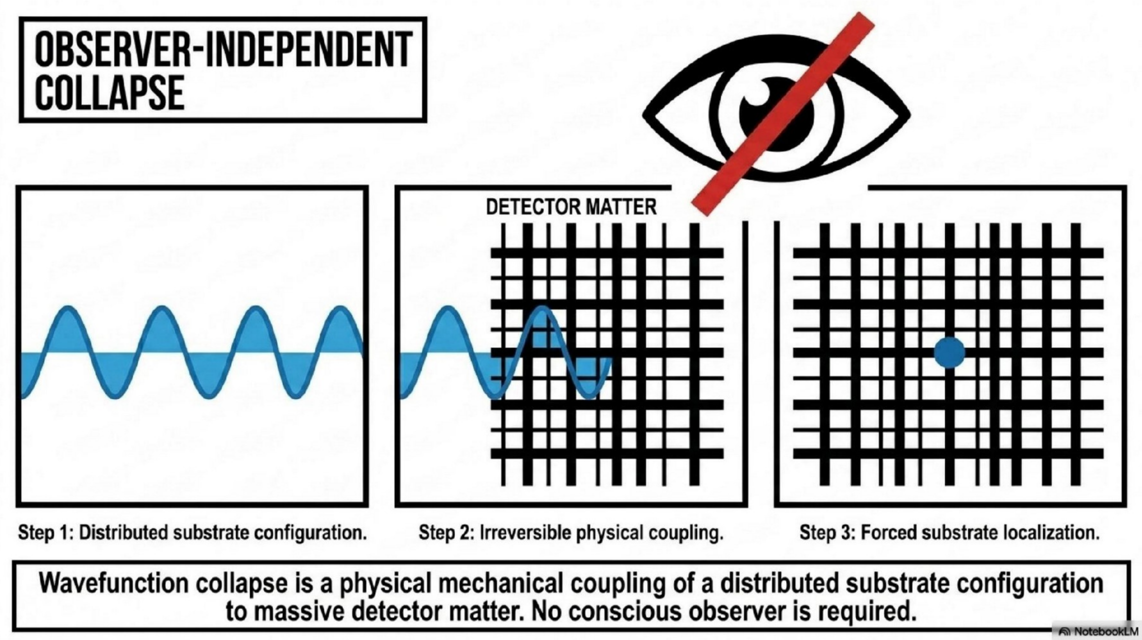

Figure 16: X: Observer-independent collapse. Wavefunction collapse is caused by irreversible physical coupling between a distributed substrate configuration and detector matter. No conscious observer is required.

The Paperweight Experiment: A Physical Clarification of the Observer Effect

The standard double-slit experiment has been used for decades to promote the idea that consciousness or observation plays a causal role in determining physical reality. Statements such as "the particle knows it is being watched," "observation collapses the wave function," and "measurement changes the outcome" are not merely imprecise. They are physically wrong, and their continued repetition in popular science, academic philosophy, and even some physics pedagogy represents a failure to follow the experimental evidence to its actual conclusion.

Place a paperweight, an inert, non-recording, structurally ordinary piece of matter with no sensing capability, no readout mechanism, no electronics, no memory system, and no connection to any observer, at one slit of a double-slit apparatus. The same argument applies if the paperweight is replaced with any other passive physical structure: a fragment of rock, a neutral scatterer, a passive atom cloud, unpowered material shielding, or any ordinary matter capable of physically coupling to the propagating particle state.

Do not attach a detector. Do not connect any electronics. Do not extract or record which-path information. Leave the apparatus untouched for hours, years, or indefinitely. Examine the screen afterward by any means, through any instrument, at any later time, or never examine it at all.

The interference pattern will be fully or partially suppressed depending on the strength and irreversibility of the physical coupling.

The paperweight has no consciousness. It performs no semantic analysis. It communicates nothing to any observer. It makes no decision. No conscious being is required to be present at any stage. No information is extracted, stored, or transmitted. Yet the interference structure is suppressed or destroyed in direct proportion to the strength and irreversibility of the interaction. The physical presence of interacting matter at the slit is sufficient. Nothing else is.

This is not a subtle or contested result. It follows directly from the mechanics of physical interaction. The propagating particle state interacts with matter at the slit. That interaction alters the coherence structure of the propagation state before the particle reaches the screen. The screen result is determined at the moment of that physical coupling. What any observer does or does not do afterward is causally irrelevant to what is already written on the screen.

The reverse configuration confirms this with equal force. Remove the paperweight and all interacting matter from both slits. Leave the apparatus entirely unobserved for any duration. When the screen is eventually examined, the interference pattern is fully intact. The timing of observation is causally irrelevant. The sophistication of the observer is causally irrelevant. The existence of any consciousness anywhere near the apparatus is causally irrelevant. What determines the outcome is whether a physical interaction occurred along the propagation path. That is all.

Such interpretations become difficult to reconcile with the experimentally demonstrated role of ordinary physical interaction in coherence suppression. The paperweight, an inert piece of matter with no sensing capability, collapses the interference pattern without any consciousness involved. Physical coupling between the propagating state and the matter at the slit is sufficient.

This also resolves a persistent conceptual confusion. The critical issue is not blocking in the ordinary macroscopic sense. The same principle applies even when the interaction is weak, partial, or non-destructive. Any irreversible physical interaction capable of coupling to the propagating state disrupts the coherent interference structure. The degree of disruption scales with the degree of irreversibility of the coupling: full irreversible coupling collapses the fringes completely; partial coupling suppresses them proportionally. This gradation is experimentally confirmed and has no natural explanation in consciousness-based accounts, which provide no mechanism for partial collapse scaling continuously with the physical strength of an interaction that no conscious observer witnesses.

Within BFUT, this follows naturally from the substrate interpretation. The particle is a propagating substrate condensation within the Spaticle field. The paperweight is a stable substrate condensation structure. When the propagating condensation encounters matter at the slit, substrate-level coupling occurs. This interaction alters the coherent propagation geometry of the multi-path state and forces localisation into a physically constrained outcome. The process is causal, mechanical, and entirely independent of whether any observer ever becomes aware of it. The screen pattern is determined at the moment of substrate interaction, not at the moment of human observation, not at the moment of information extraction, and not at the moment any mind chooses to look.

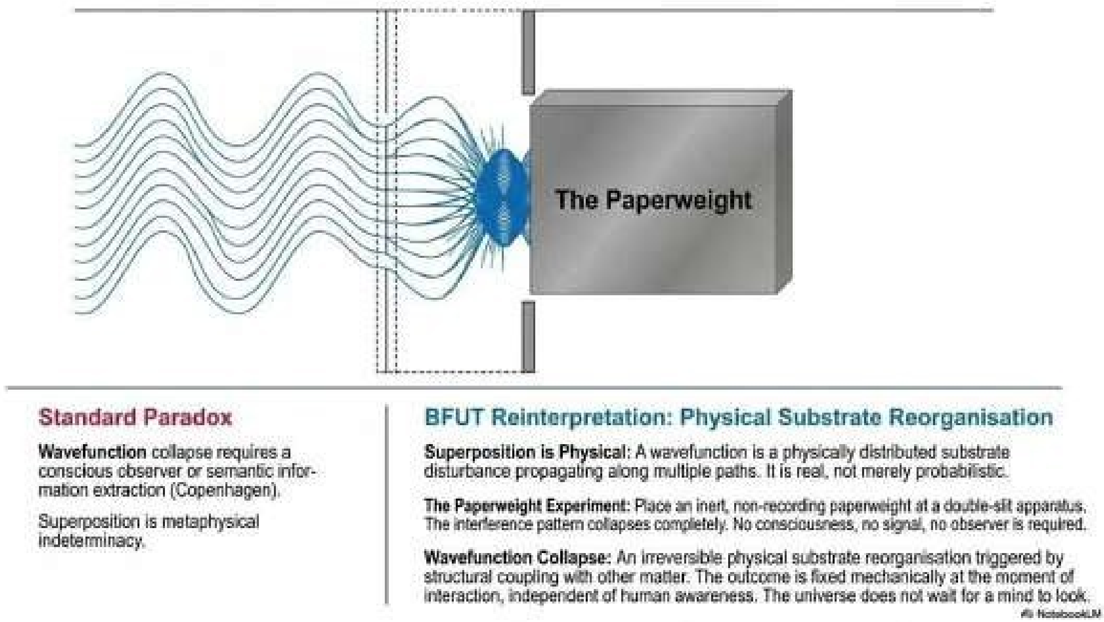

Figure 17: Physical substrate reorganisation during measurement. Irreversible interaction with matter alters coherent substrate propagation and produces definite outcomes without requiring conscious observation.

Testable Prediction

The physical-interaction interpretation generates a direct experimental prediction distinguishing it from consciousness-based collapse models and from stronger information-theoretic interpretations of quantum mechanics.

Place an inert, non-recording physical object at one slit of a double-slit apparatus. The object may be a paperweight, rock fragment, passive material structure, neutral scatterer, weak interaction medium, or any ordinary physical matter capable of coupling to the propagating state. Ensure that no detector is attached, no electronics are connected, no signal is transmitted, and no observer interacts with the system during propagation.

Run the experiment and examine the screen afterward by any means or at any later time. The BFUT prediction is that the interference pattern will be suppressed in direct proportion to the strength and irreversibility of the physical coupling. Strong irreversible coupling drives fringe visibility toward zero within experimental precision, while weaker coupling produces proportionally partial suppression.

If interference persists despite confirmed physical interaction between the propagating state and inserted matter, the physical-interaction account fails. Such a result would require either that the matter was effectively transparent at the relevant interaction scale, or that physical interaction itself is insufficient to disrupt coherent propagation. Both are independently testable and would constitute a genuine discovery and not a validation of consciousness-based accounts.

The experiment sharply distinguishes physical-interaction models from consciousness-dependent accounts. Any interpretation assigning causal significance to awareness, observation, or semantic information extraction predicts that interference should persist when no conscious observer, detector, or readable record exists. The physical-interaction account predicts that physical coupling alone is sufficient, with the degree of interference suppression scaling continuously with the strength and irreversibility of the interaction. A paperweight in the dark with no one watching produces the same result as a sophisticated quantum detector read by a Nobel laureate. The particle does not know the difference because there is no difference to know. The interaction is physical. The outcome is physical. The rest is a human narrative imposed on a process that was never waiting for a mind to complete it.

The experiment also constrains stronger information-theoretic interpretations. Suppose the interaction leaves no recoverable record because the paperweight is immediately melted, randomised, vaporised, or physically destroyed before any inspection is possible. The physical-interaction account predicts that the interference pattern remains absent because the substrate interaction already occurred at the slit. The outcome at the screen was fixed by the physical coupling event itself, not by the later survival or accessibility of information about that event. The universe does not wait to see whether someone can in principle recover the record before deciding what happened.

The graded prediction is a further discrimination. Partial physical coupling, a weak scatterer, a dilute atom cloud, a grazing interaction, produces partial suppression of the interference fringes proportional to the strength of the physical coupling. This is continuously variable and requires no threshold of consciousness, no threshold of information completeness, and no threshold of observer sophistication. It scales with physics alone. Consciousness-based and information-theoretic accounts have no natural mechanism to reproduce this continuous gradation in the regime where no observer and no readable record exist at any stage.

In BFUT terms, collapse is not an informational abstraction, not a philosophical puzzle, and not evidence that minds shape reality. It is a physical substrate-level transition produced by interaction between organised condensation structures within the Spaticle field. The experimental evidence is naturally explained once irreversible physical interaction itself is recognised as sufficient to produce coherence suppression and localisation.

16. Superposition as Distributed Physical Propagation

Superposition: Standard account

In standard quantum mechanics, superposition is usually described mathematically but left physically undefined. A quantum system is said to exist in multiple possible states simultaneously until measurement occurs. Popular interpretations often extend this into claims about parallel realities, many worlds, or reality remaining fundamentally undefined before observation.

BFUT Account

BFUT gives a direct physical interpretation. A particle is not treated as a tiny point moving along one hidden path. It is a distributed organised disturbance propagating through the Spaticle

substrate. The wavefunction represents the real spatial distribution of this propagating substrate organisation.

Superposition therefore does not mean multiple universes, multiple particles, or simultaneous completed realities. It means that the propagating substrate disturbance remains physically distributed across multiple possible interaction paths before irreversible interaction occurs. The wavefunction therefore represents a physically distributed substrate disturbance and not a mere mathematical bookkeeping device or expression of observer knowledge.

The distributed propagation is physically real because the distributed regions can interfere with one another. This is experimentally observable in double-slit interference, neutron interferometry, electron interference, and quantum computing itself. Interference is impossible if the distributed propagation state is merely ignorance about a hidden classical trajectory. Something physically distributed must exist prior to detection. The distributed propagation state is therefore physically real even before localisation occurs.

Different regions of the distributed state carry different deformation intensity, coherence strength, and interaction probability. As the disturbance propagates, these regions evolve continuously according to substrate propagation dynamics. Regions can reinforce one another constructively or suppress one another destructively.

Measurement does not create reality. Measurement is the irreversible physical interaction between the distributed propagating disturbance and another organised substrate structure such as a detector. Once stable irreversible coupling occurs at one location, the prior distributed propagation configuration no longer persists as an independently evolving coherent state.

BFUT therefore does not require parallel realised universes to explain distributed propagation and interference phenomena. Superposition represents physically distributed propagation within the substrate, not metaphysical indeterminacy.

Quantum Entanglement, Bell Correlations, and Finite Interaction Domains

What the interpretation states as Shared Substrate Configuration

When two particles interact and are then separated, measurements on one particle instantaneously affect the state of the other, regardless of the distance between them. This non-local connection has been confirmed by Bell inequality violation experiments, including work recognised by the 2022 Nobel Prize in Physics awarded to Aspect, Clauser, and Zeilinger.

BFUT Account as Shared Substrate Configuration

Quantum entanglement is widely interpreted as evidence for non-local behaviour in nature. BFUT agrees with the observed experimental correlations but rejects the interpretation that they require instantaneous communication across space.

The BFUT explanation begins with a simple principle: correlation does not imply ongoing communication. When two particles emerge from a common formation event, they originate as components of a single substrate configuration. Their subsequent properties are therefore not independent. Correlations observed later need not be generated at the moment of measurement because the relevant structural information was already established during the original interaction.

A useful analogy is two bubbles generated simultaneously within a fluid. The bubbles may possess matching properties because they originated from the same event. Measuring one bubble does not cause the second bubble to change. The correlation exists because both inherited common structural conditions from their formation history. The same principle applies to quantum systems. Correlations can arise from shared substrate organisation without requiring any superluminal signal between separated particles.

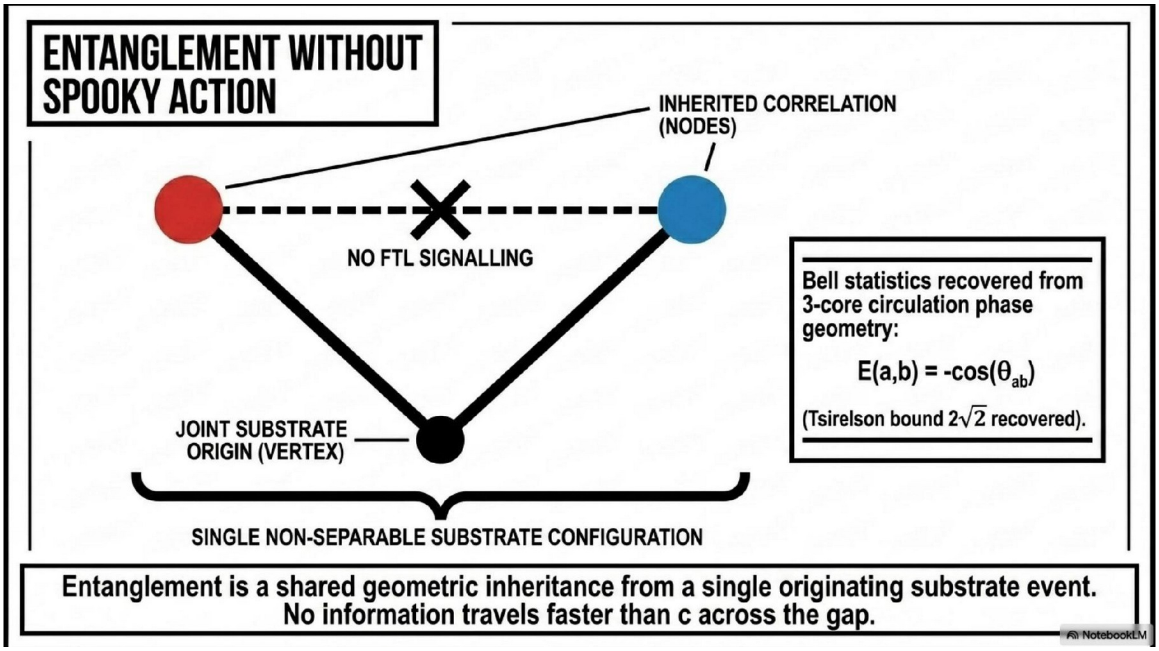

Figure 18: Entanglement without spooky action. Correlations arise from shared geometric inheritance from a single originating substrate event. No information travels faster than c.

Bell's Theorem and Inequality Violations as Shared Substrate Configuration

Bell's theorem demonstrated that no theory based on independent local hidden variables can reproduce the full statistical correlations observed in entanglement experiments. The 2022 Nobel Prize in Physics recognised experimental confirmation through the work of Clauser, Aspect, and Zeilinger. These experiments are frequently misunderstood as proving faster-than-light communication, instantaneous signalling, or observer-created reality. They prove none of these things.

What Bell inequality violations actually demonstrate is that the measured systems cannot be treated as fully independent local objects possessing separable pre-existing local states. BFUT fully agrees with the experimental results while giving them a different physical interpretation. The entangled system begins as one shared substrate configuration. The separated components inherit correlated structural constraints from that original unified configuration. Bell's assumption of separable local independence therefore does not apply from the beginning.

The experiments disprove independent local hidden-variable models. They do not require superluminal communication. No signal needs to travel between particles during measurement because the correlation already exists within the shared substrate organisation established during the original interaction. BFUT does not restore classical independent local hidden variables. The shared substrate configuration itself is physically extended and globally constrained from the moment of joint formation. The measured correlations are therefore manifestations of persistent substrate-level structural continuity and not instantaneous communication across space.

This also explains why entanglement cannot transmit usable information faster than light. The observer cannot freely control the local measurement outcome. Only after classical comparison between observers do the correlations become visible. The correlations are built into the shared substrate structure itself and not transmitted dynamically during measurement.

More fundamentally, BFUT predicts that no physical mechanism can transmit information faster than the substrate propagation limit c. This statement is independent of entanglement itself. Even if two systems possess correlated histories, any new influence, signal, instruction, or transferable information remains constrained by the substrate propagation budget. Faster-than-light information transfer is therefore forbidden as a consequence of the substrate dynamics and not as a special property of entanglement.

Finite Interaction Domains and the DDR Relation as Shared Substrate Configuration

BFUT further predicts that all physical interactions possess finite domains. This follows from the finite density of the Spaticle field and from the DDR deformation-domain relation derived independently in BFUT Paper 18:

$$R_d = (3M / (8\pi\rho_s))^{1/3}$$

Here M is the mass of the organised substrate structure and $\rho_s = 7.3 \times 10^{-27}$ kg/m³ is the adopted equilibrium density. The same DDR relation applies from elementary-particle to galactic masses.

Object: DDR Domain Radius

Proton: 0.301 m (proton mass dominates)

Hydrogen atom: 0.301 m (proton mass dominates)

Earth: 4.87 light years

Sun: 337 light years

Milky Way: 872 kpc (for 6×10^{11} M☉)

The existence of a single deformation-domain relation spanning quantum and astrophysical scales is one of the central unifications of BFUT, linking quantum-scale persistence and astrophysical gravitational structure through the same substrate dynamics. The full DDR derivation is presented in BFUT Paper 18 (DOI: 10.5281/zenodo.20145506). The validation across 190 systems and the associated numerical simulations are presented in BFUT Paper 25 (DOI: 10.5281/zenodo.20535295).

Consequently, any apparent entanglement correlation may arise from common-origin substrate organisation, shared environmental influence, electromagnetic interaction, gravitational interaction, or any other finite-domain physical mechanism. None of these require non-local communication. The decisive test concerns direct controllable influence. If particle A is deliberately manipulated and particle B, separated beyond all applicable physical domains, exhibits a corresponding response that cannot be explained through common origin, shared environment, electromagnetic coupling, gravitational coupling, or any other finite-domain interaction, then the BFUT interpretation would be falsified.

BFUT therefore makes a clear prediction: correlations originating from common substrate organisation may persist, but no experiment will demonstrate controllable non-local influence beyond all available physical interaction domains. Continued failure to produce such influence supports the interpretation that entanglement reflects inherited substrate correlations and not genuine action at a distance.

17. The Many-Worlds Interpretation

What the interpretation states

Hugh Everett proposed in 1957 [3] that the Schrödinger equation applies universally and without exception. When a measurement occurs, the universe does not collapse to one outcome. Instead it branches: every possible outcome occurs in a different branch of a continually splitting universal wavefunction. All branches are equally real. There is no collapse. There is only the universal wavefunction evolving deterministically.

BFUT Account

Many-worlds arises because the Schrödinger equation, taken as a fundamental law without a physical substrate, provides no mechanism for selecting one outcome at measurement. If the equation must apply everywhere and always, branching appears to be the only self-consistent interpretation. In BFUT, the Schrödinger equation is not a fundamental law. It is a low-energy approximation to the substrate propagation dynamics. The substrate has a defined physical mechanism for measurement: the irreversible threshold-crossing that fixes one configuration. There is no branching because there is a physical selection process. Many-worlds is therefore not required in BFUT.

BFUT does not assert that other branches do not exist in any metaphysical sense. It asserts that the substrate dynamics provide a physical mechanism for unique outcome selection that makes branching unnecessary as a physical postulate.

18. Schrödinger's Cat

What the interpretation states

Erwin Schrödinger proposed in 1935 a thought experiment to illustrate what he saw as an absurdity in the Copenhagen interpretation. A cat is placed in a sealed box with a quantum device that has a 50 percent probability of triggering a poison. According to Copenhagen, until the box is opened, the cat is in a superposition of alive and dead states. Schrödinger intended this as a reductio ad absurdum: surely cats are not in superpositions.

BFUT Account

The Schrödinger's cat situation does not produce a cat in superposition within BFUT. The quantum device interacts with the surrounding apparatus, which consists of macroscopic numbers of condensations. The substrate deformation of the quantum event propagates through the apparatus and reaches coherence-threshold irreversibility long before it reaches the cat. The cat's fate is fixed by the irreversible substrate reorganisation of the apparatus, which occurs at the quantum event. The cat is always in one definite state from the moment the quantum event occurs. The superposition does not extend to macroscopic objects because macroscopic objects consist of so many condensations that any coherent superposition is destroyed by the collective substrate interactions almost instantaneously. This is consistent with decoherence theory and with the BFUT account of measurement as threshold crossing.

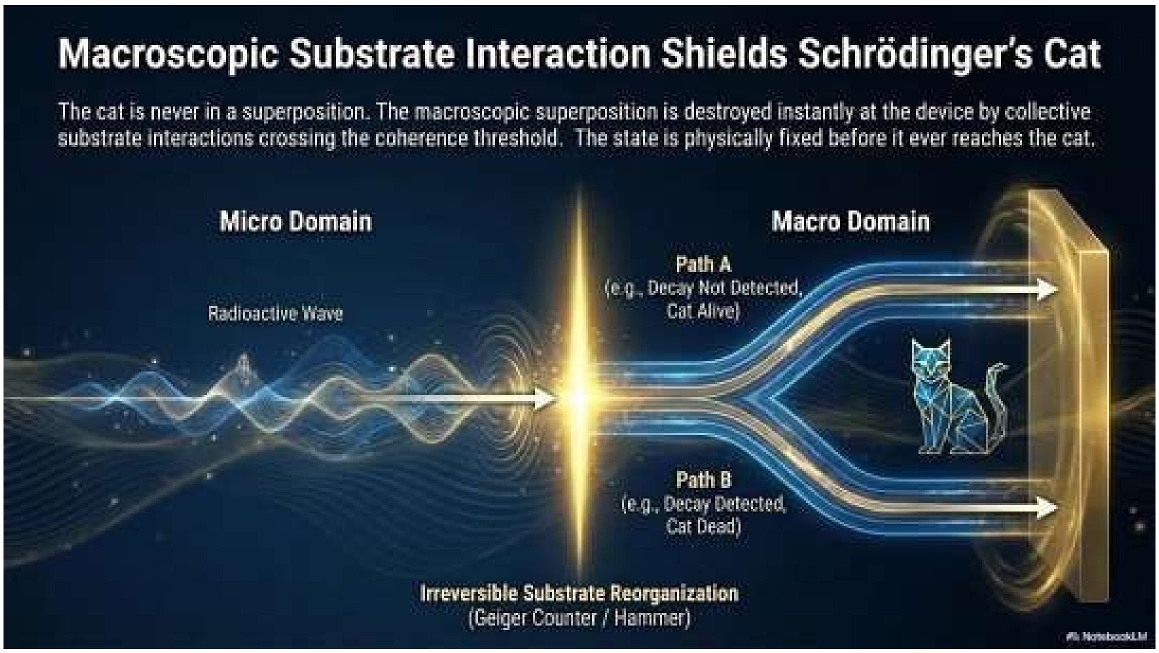

Figure 19: Schrödinger's Cat lives…. for now

19. Zero-Point Energy and Vacuum Fluctuations
What the interpretation states

Quantum field theory predicts that the vacuum is not empty. Every quantum field has a ground state energy of one-half $\hbar*\omega$ per mode, even when no particles are present. These zero-point fluctuations have measurable consequences, most notably the Casimir effect: two uncharged conducting plates placed close together experience an attractive force because the vacuum fluctuations between them are restricted to fewer modes than outside. Some proponents have suggested that zero-point energy could be extracted as a usable energy source. The BFUT framework identifies two errors in the standard QFT vacuum energy treatment - multiplicity of independent fields where there is physically one, and zero-point energy assigned to empty modes - whose correction collapses the enormous QFT prediction directly to $\rho_s \cdot c^2$, resolving the cosmological constant problem.

BFUT Account

In BFUT, the vacuum is physically occupied by the Spaticle substrate at density ρ_s. The substrate is never empty. What QFT calls vacuum fluctuations are transient local perturbation modes of the substrate that do not reach the stability threshold required for a persistent condensation. They are real physical oscillations of the substrate, not mathematical artefacts. The Casimir effect is a real physical consequence: when two conducting plates restrict the boundary conditions of the substrate between them, fewer perturbation modes can exist in that region. The energy of the restricted substrate configuration is lower than the unrestricted configuration. The plates are drawn together by the pressure difference. This is a straightforward mechanical consequence of the substrate having structure, with no need to invoke particles appearing from nothing.

The extraction of zero-point energy as a usable power source is not supported within BFUT. The substrate is at its equilibrium density ρ_s. Extracting energy from the substrate would require reducing the substrate below its equilibrium density, which would require work against the substrate pressure. The net energy available is zero. The Casimir force is real but it reflects the geometry of the boundary conditions, not a reservoir of extractable free energy.

20. Quantum Tunneling

What the interpretation states

A quantum particle can pass through a potential energy barrier that classical physics says it cannot cross, because its total energy is less than the barrier height. The probability of tunneling falls exponentially with barrier width and height. Tunneling is responsible for α decay in nuclear physics, the operation of tunnel diodes, and scanning tunneling microscopes.

BFUT Account

In BFUT, a potential barrier is a region of elevated substrate deformation energy. A condensation approaching a barrier has a substrate deformation field with a finite spatial extent set by the coherence length of the deformation. If the barrier width is comparable to or smaller than the coherence length, the deformation field has nonzero amplitude on the far side of the barrier. The condensation does not pass through the barrier material. The substrate deformation reorganises continuously across the barrier when the geometry permits it. The tunneling probability is determined by the ratio of the barrier width to the coherence length of the substrate deformation: wider barriers relative to the coherence length produce exponentially smaller tunneling probability, consistent with the quantum mechanical result.

This is a physical account of tunneling with no mysterious element. The condensation does not violate energy conservation and does not travel faster than c. The substrate simply reorganises continuously, and if the geometry of the barrier allows continuity of the deformation field across it, the condensation appears on the far side.

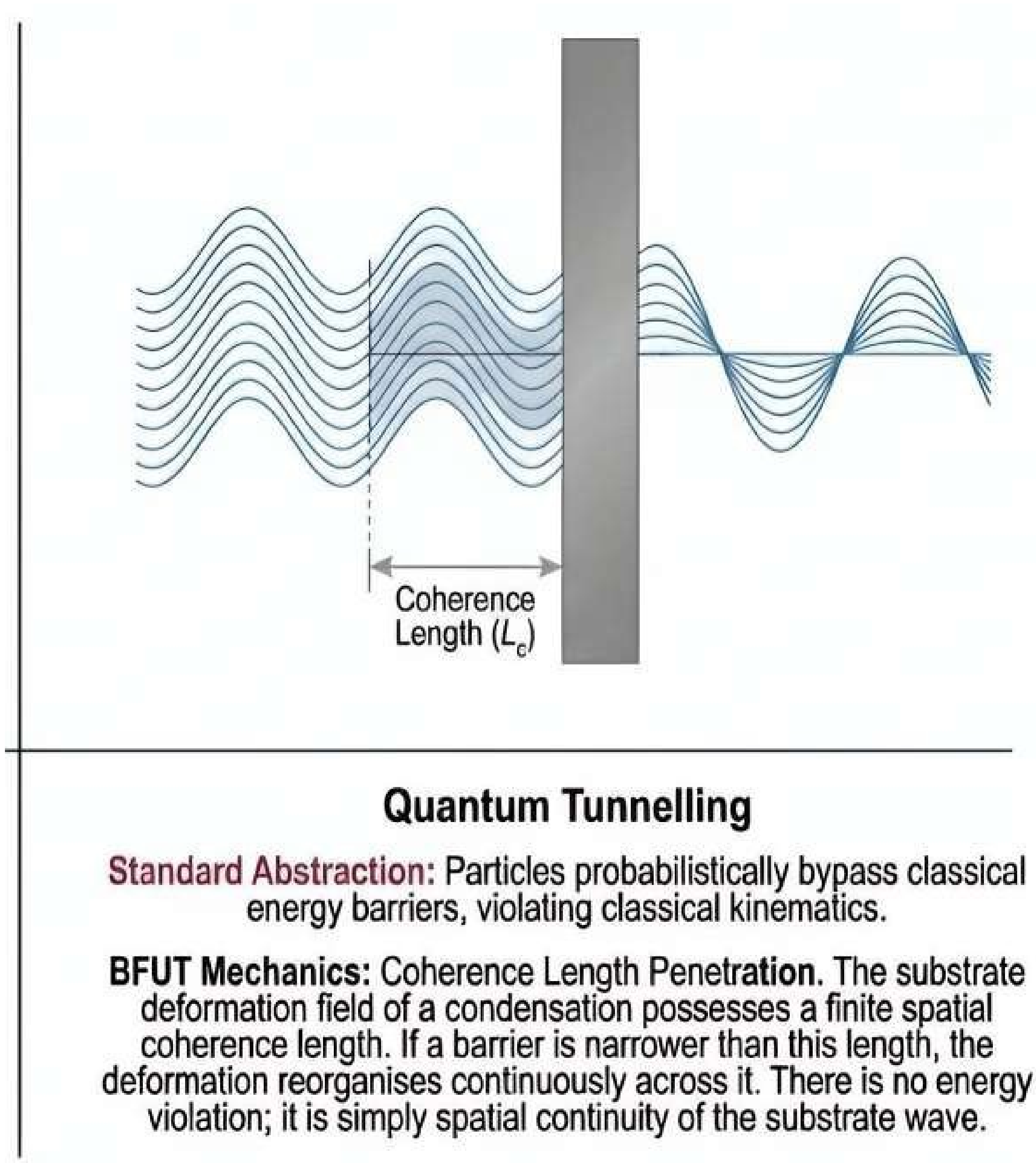

Figure 20: Quantum tunnelling is not mysterious

21. Decoherence and the Quantum-to-Classical Transition

What the interpretation states

Quantum Tunnelling: Explicit BFUT Form of the Decay Constant

The substrate reinterpretation of tunnelling above gives the decay constant the following explicit form when the BFUT ħ_vss = mp·c·rp/(π·R_0) is substituted into κ_vss = √[2m(V−E)]/ħ_vss:

$$\kappa = \pi \cdot R_0 \cdot \sqrt{2m(V-E)} / (m\_p \cdot c \cdot r\_p)$$

The penetration depth 1/κ is the condensation length rp/(π·R_0) divided by the dimensionless ratio √(2m(V−E))/(mp·c): the ratio of the barrier energy scale to the proton momentum scale. For the condensation effective mass m_eff = 5.324 × 10^{-28} kg (not the electron mass 9.109 × 10^{-31} kg) and a 1 eV barrier: 1/κ_vss = 8.08 pm. That is the ħ substitution only, about 0.00048%. A real electron at the same 1 eV barrier has 1/κ ≈ 195 pm. The tunnelling probability T = exp(−2κ_vss d) in BFUT form:

$$T = \exp(-2\pi \cdot R_0 \cdot d \cdot \sqrt{2m(V-E)} / (m\_p \cdot c \cdot r\_p))$$

Tunnelling is universal because every condensation has a characteristic penetration depth set by the same condensation scale rp/(π·R_0).

De Broglie Wavelength from Substrate Condensation Scale

The de Broglie wavelength is λdB_vss = h_vss/p = 2πħ_vss/p. Substituting BFUT ħ_vss:

$$\lambda dB\_vss = mp \cdot c \cdot rp / (\pi \cdot R_0 \cdot p)$$

Wave-particle duality is the ratio between the particle momentum p and the condensation momentum scale mp·c, modulated by the condensation length rp/(π·R_0). For a 100 eV electron, p = √(2 m_e E) gives λ = h/p ≈ 122.6 pm. With the same p, λ differs from the standard value by the ħ substitution only, about 0.00048%. Every interferometric prediction that depends on λ inherits that 0.00048% ħ shift.

Quantum Harmonic Oscillator Energy Levels from Condensation Circulation

Energy levels E_n_vss = (n+1/2)ħ_vssω. With BFUT ħ_vss:

$$E\_n\_vss = (n + 1/2) \cdot mp \cdot c \cdot rp \cdot \omega / (\pi \cdot R_0)$$

The ground state energy E_0_vss = ħ_vssω/2 is the minimum internal circulation energy of a condensation oscillating at frequency ω. At the proton Compton frequency ω = c/rp: E_0 = mp·c^2/(2π·R_0) = 117.5 MeV. The factor n+1/2 reflects n full circulation quanta above the minimum half-quantum Lmin = ħ_vss/2 required by the 720° topology. Zero-point energy belongs to organised condensations, not to empty field modes.

Quantum decoherence is the process by which quantum superpositions are destroyed through interaction with the environment. It explains the transition from quantum to classical behaviour without requiring a special role for observers or measurement.

Decoherence as Environmental Substrate Coupling

One of the central questions of quantum mechanics is why coherent quantum behaviour disappears in large systems and ordinary macroscopic reality appears classical. Standard treatments describe decoherence mathematically as loss of phase coherence caused by environmental interaction. While the mathematics is successful, the physical picture is often left abstract. BFUT provides a direct physical interpretation.

A coherent quantum state is an organised propagating substrate configuration. To maintain coherence, the distributed propagation structure must remain isolated from irreversible environmental interaction. The environment is not passive emptiness. It consists of enormous numbers of surrounding substrate condensations continuously interacting through electromagnetic, thermal, vibrational, and material coupling processes.

As environmental interaction increases, the organised propagation structure becomes progressively disrupted, phase relationships become unstable, distributed propagation paths cease evolving coherently, and irreversible substrate coupling begins dominating the system dynamics. This process is decoherence. Decoherence therefore reflects progressive loss of coordinated substrate organisation through environmental coupling and not conscious observation.

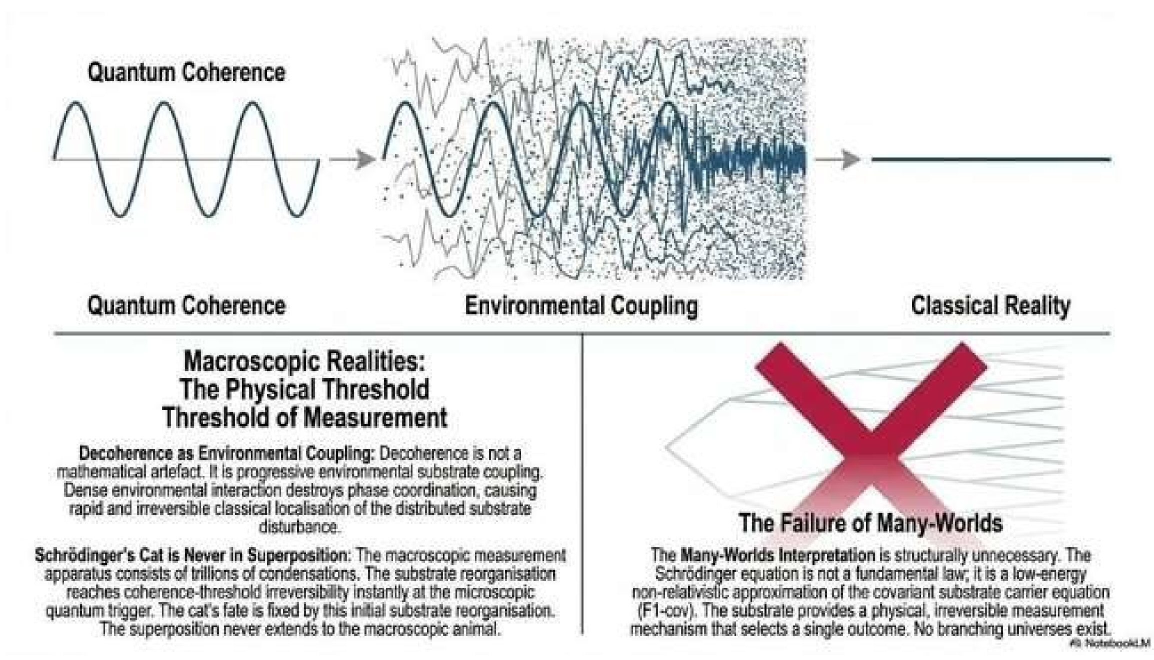

Figure 21: Environmental coupling progressively disrupts coherent substrate organisation, producing irreversible

decoherence and classical localisation.

The transition is gradual and not sudden. Weak environmental interaction produces partial coherence suppression. Strong irreversible coupling produces rapid classical localisation. This explains why isolated electrons can maintain interference, larger molecules decohere more easily, macroscopic systems classicalise extremely rapidly, and quantum computing requires extreme isolation, shielding, cryogenic cooling, and noise suppression.

The issue is not consciousness. The issue is physical interaction. A coherent quantum state is fragile because distributed substrate organisation must remain dynamically coordinated across the propagation structure. Environmental coupling progressively destroys that coordination. Classical reality therefore emerges naturally from irreversible environmental embedding and not from a mysterious boundary between quantum and classical physics.

22. The Quantum-to-Classical Transition

Progressive environmental embedding

One of the longstanding problems in physics is understanding why microscopic systems display distributed quantum behaviour while macroscopic systems appear localised and classical. BFUT explains this transition through progressive environmental embedding.

Small isolated systems can maintain coherent distributed substrate organisation because environmental coupling remains limited. Their propagation structures remain isolated to preserve interference and phase stability. As systems grow larger, environmental interaction cross-sections increase, internal coupling complexity increases, thermal interaction increases, and irreversible substrate interaction becomes progressively unavoidable. The system therefore becomes increasingly embedded within surrounding substrate organisation.

Distributed coherent propagation gradually gives way to stable localised interaction structures. Classical behaviour emerges naturally from the loss of coherent distributed propagation. There is therefore no sharp boundary separating quantum and classical reality. The transition is continuous and depends on environmental coupling, coherence persistence, interaction irreversibility, substrate embedding, and system organisation scale.

Quantum mechanics and classical mechanics are therefore different behavioural regimes of the same underlying substrate dynamics and not fundamentally separate domains of reality.

23. Retrocausality and Backward-in-Time Signalling

What the interpretation states

Some interpretations of quantum mechanics, including the transactional interpretation [6] of John Cramer, suggest that quantum events involve advanced waves propagating backward in time as well as retarded waves propagating forward. Some researchers have proposed that the correlations in delayed-choice experiments indicate that future measurement settings can affect past particle states. Retrocausal interpretations have been advocated by serious physicists including Huw Price and Rod Sutherland.

BFUT Account

BFUT Account The physical basis of the BFUT arrow of time is developed in BFUT Paper 19. Time is interpreted as substrate evolution and not motion through a pre-existing time dimension. Because the substrate evolves through irreversible propagation processes, closed timelike curves have no physical implementation mechanism within BFUT. A closed timelike curve would require a physical substrate disturbance to return to an earlier substrate configuration already incorporated into the accumulated evolution history of the system. The BFUT framework provides no mechanism by which this can occur. GR solutions that formally contain closed timelike curves are therefore interpreted as mathematical solutions of an effective spacetime description and not physically realisable states of the substrate. Hawking's chronology protection conjecture is consistent with this interpretation and receives a physical substrate basis within BFUT. Retrocausal influence would require a substrate disturbance to propagate in the direction of decreasing time, against the physical propagation direction. The substrate provides no mechanism for this. Delayed-choice experiments, in which the measurement setting is determined after the particle is emitted, are consistent with BFUT without retrocausality: the substrate deformation geometry of the particle evolves continuously from emission to detection, and the measurement setting at detection determines which aspect of that geometry becomes irreversibly fixed. The geometry was always there. No signal travels backward in time.

24. Quantum Immortality

What the interpretation states

Quantum immortality is a philosophical extension of the many-worlds interpretation. If every quantum event produces branching, and if consciousness selects the branch in which it continues to exist, then a conscious observer can never experience their own death: there is always some branch in which they survive. Max Tegmark [4] and others have discussed this as a logical consequence of many-worlds combined with the role of the observer.

BFUT Account

Quantum immortality as stated requires two premises: many-worlds branching and consciousness as the branch selector. BFUT rejects both. Many-worlds branching is unnecessary because the substrate provides a physical measurement mechanism that selects one outcome. Consciousness is not a branch selector: it is a property of mass, not a force that determines quantum outcomes. The argument for quantum immortality therefore does not arise within BFUT. Physical death corresponds to the irreversible disorganisation of the condensation structure that sustains a given level of consciousness. The substrate matter continues to exist and retains its minimal consciousness (CIfloor). The organised condensation structure that constituted the individual does not continue.

25. The Simulation Hypothesis

What the interpretation states

Nick Bostrom proposed in 2003 [5] that if civilisations with sufficient computational power are likely to simulate conscious beings, and if there are many such civilisations, then the fraction of conscious beings living in simulations vastly exceeds those living in the base reality. Therefore, the probability that any given conscious being is in a simulation may be high. Elon Musk and others have popularised this as a serious possibility. Some physicists have noted that the digital structure of certain physical quantities, such as the Planck length, is consistent with a simulation interpretation.

BFUT Account

The simulation hypothesis requires a substrate external to the observable universe from which the simulation is run. BFUT establishes through the closed-container argument that the observable universe is causally closed: nothing enters from outside. A simulation running from outside would require causal influence from outside, which is ruled out. Additionally, BFUT derives particle-sector quantities from the condensation structure and its associated anchors rather than treating them as arbitrary simulation parameters.

Light, Massless Propagation, and the Physical Origin of the Universal Speed Limit

One of the deepest questions in physics is not why light travels at speed c, but why so many apparently different phenomena share exactly the same propagation speed: electromagnetic radiation, gravitational waves, massless gauge excitations, and causal influence. These originate from different mathematical sectors of physics yet all propagate at c. Within the BFUT framework this coincidence is neither accidental nor fundamental. The quantity c is the maximum propagation and reorganisation rate of the Spaticle substrate itself.

The Spaticle field is the physical medium through which all organised structure, force transmission, and information propagation occur. Every physical process requires local substrate reorganisation. The finite compressibility, density, and propagation capacity of the substrate impose a maximum physically achievable propagation rate. This limiting rate is observed experimentally as c. The universal speed limit therefore exists because no physical process can reorganise the substrate faster than the substrate can propagate causal information through itself. The speed c is a property of the substrate, not a property of photons.

Light propagates at c because photons represent freely propagating organised excitations of the substrate that do not require the maintenance of a stable localised condensation structure. Their energy is devoted entirely to propagation. They therefore travel at the maximum propagation rate permitted by the substrate. The same reasoning is used in BFUT to explain why gravitational waves propagate at c. In the BFUT framework, gravitational waves are propagating deformation disturbances of the Spaticle field. Since the disturbance propagates through the same substrate that defines c, the propagation speed must equal c. Within BFUT, the equality of gravitational-wave and light propagation speeds follows from their common substrate propagation mechanism; this is a framework-level explanation, not an additional empirical measurement.

The distinction between massless and massive particles follows directly from substrate organisation. A massless excitation devotes its entire energy budget to propagation. A massive particle must continually maintain a localised condensation structure within the substrate. Part of its available energy is committed to maintaining organisation and not pure propagation. The propagation velocity consequently falls below c. This explains why neutrinos travel extremely close to c. Neutrinos possess very small but non-zero mass and require only minimal substrate localisation. Almost their entire energy budget remains available for propagation. Their velocities therefore approach c while remaining slightly below it, consistent with observation.

Within this framework, light does not define the universal speed limit. The universal speed limit defines the behaviour of light. Photons, gravitational waves, electromagnetic disturbances, and all other massless excitations share the same speed because they are manifestations of one underlying propagation constraint: the finite propagation capacity of the Spaticle field determines the maximum rate at which organised physical reality can evolve. A dedicated paper developing this framework in full is in preparation.

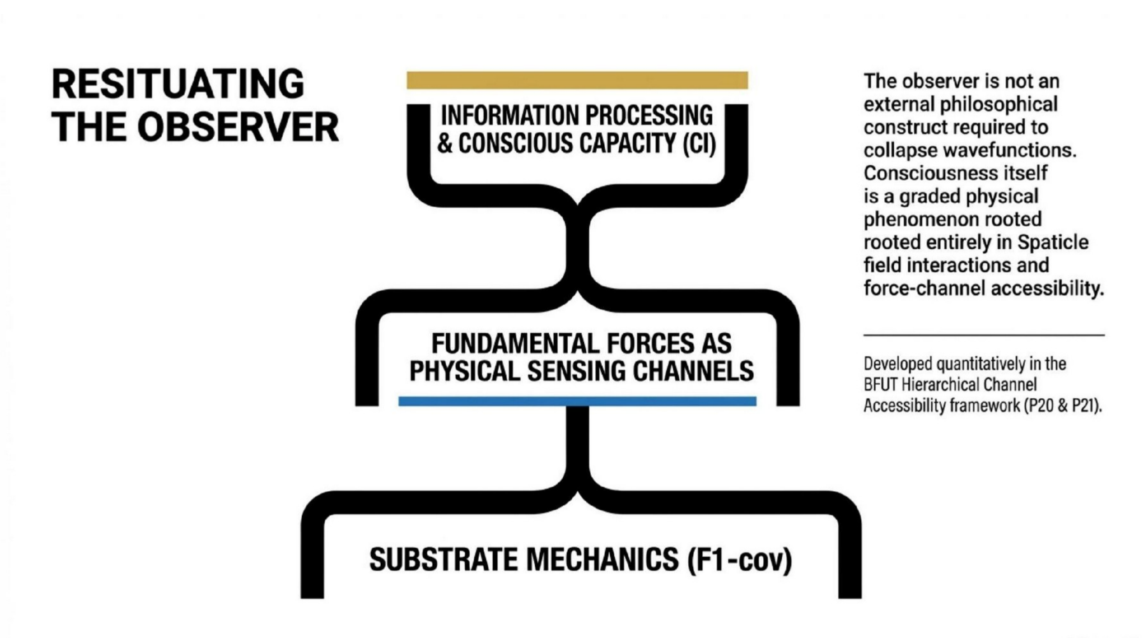

Figure 22: Resituating the observer. Consciousness is a graded physical phenomenon rooted in substrate interactions and force-channel accessibility, not an external entity required to collapse wavefunctions.

The complete derivation, calibration, and application to 100 species is provided in BFUT Paper

21. One result is worth stating here because it bears on the interpretation of human consciousness: several non-human species, including the dolphin (CI_0 = 123.9), the crow (CI_0 = 115.7), and the chimpanzee (CI_0 = 113.9), exceed the average human in intrinsic structural capability. The formula, run on biologically motivated parameters, produces this result because the biology warrants it. The effective CI of the human average is 100 because the human survival factor S = 1.00, which no other species achieves. This is the interpretation reported by the cited BFUT framework.

26. Forward Reference to Papers 20 and 21

The full formal derivation of the HCA framework, sensing conditions, and the Consciousness Index formula and dataset are provided in BFUT Papers 20 and 21. The present section states only what is directly relevant to the quantum interpretation programme of this paper.

The Observer and Consciousness: Bridge to BFUT Papers 20 and 21

Quantum mechanics inevitably raises the question of the observer. Many interpretations invoke consciousness, observation, information, or awareness, yet leave these concepts undefined or without physical grounding. Within the BFUT programme, the observer is not treated as an external philosophical construct. The same substrate framework used to derive particle structure, electroweak relationships, quantum behaviour, and atomic organisation is extended in BFUT Papers 20 and 21 to derive a quantitative framework for consciousness itself.

Paper 20 develops a mathematical account linking matter organisation, information processing, physical structure, and conscious capacity within the same substrate ontology used throughout the present work. Paper 21 extends this framework into a Consciousness Index that assigns numerical consciousness values across biological systems. Without species-specific adjustments, the same formalism is applied across approximately one hundred organisms spanning the biological hierarchy from viruses to large mammals, including humans and blue whales.

The resulting framework produces a quantitative ranking of conscious complexity across radically different forms of life using a single mathematical structure. This is particularly relevant to the present paper because quantum-consciousness proposals have historically lacked a quantitative definition of consciousness itself. Within the BFUT programme, the observer entering quantum mechanics is not left undefined. A mathematical framework for observer complexity, observer hierarchy, and consciousness quantification is developed separately and applied to published biological data.

The significance of this result extends beyond consciousness studies. If the same substrate framework can account for particle structure, electroweak relationships, quantum behaviour, atomic organisation, and consciousness using a common physical foundation, then the observer entering quantum mechanics is no longer an external entity introduced by interpretation. The observer becomes another organised manifestation of the same underlying substrate dynamics.

Importantly, the Consciousness Index is not intended as a result restricted to a fixed dataset. Like the DDR relation, the coherence index, and other BFUT-derived quantities, it is a predictive framework intended for continued testing. Several BFUT relations were initially developed using comparatively small datasets and subsequently applied, without modification, to much larger observational samples and entirely new systems. The same principle applies here. The Consciousness Index has been evaluated across approximately one hundred species, but the framework makes an open invitation for independent researchers to apply the same formula to additional organisms, larger datasets, and new biological domains without adjustment of the underlying formalism. The objective is not merely to explain existing rankings but to provide a framework capable of surviving extension, validation, and challenge.

The detailed derivations, validation datasets, consciousness rankings, and mathematical formalism are presented in BFUT Papers 20 (DOI: 10.5281/zenodo.19992457) and 21 (DOI: 10.5281/zenodo.20025739) and are not repeated here.

The present paper therefore addresses the quantum ontology. BFUT Papers 20 and 21 address the observer that inhabits that ontology.

27. Conclusion

BFUT Paper 19A extends the BFUT programme to quantum mechanics, the H-class radial resonance, and quantum consciousness. The Schrödinger equation is derived from substrate propagation dynamics, the Born rule from substrate energy density, and half-integer spin from the topology of embedded condensations - a BFUT physical explanation for the fermion/boson distinction based on condensation and propagation topology. BFUT proposes observer-independent collapse: physical coupling produces state resolution without requiring a conscious observer. The observed H-class state is treated as a radial resonance of the single Spaticle field, with the 124.75 GeV/c² mass derived from the P16/P19 radial condensation invariant.

Papers 14 through 19 constitute the substrate foundations of force, matter, gravitation, light propagation, time, relativistic causality, and coupling structure. Paper 19A extends that framework into quantum mechanics, Higgs physics, and quantum consciousness.

Interactive simulations of the Born rule as substrate deformation energy density, observer-independent wavefunction collapse through substrate coupling, and Bell correlations as common-origin Spaticle field inheritance without superluminal communication are available in the BFUT companion simulations code deposit (DOI: 10.5281/zenodo.20554084).

References

[1] Sharma, V. S. (2026). The Origin of Matter, Antimatter, and Fundamental Forces: How Protons, Electrons, and Hydrogen FormeD P16. Zenodo. DOI: 10.5281/zenodo.19908215

[2] Sharma, V. S. (2026). The Consciousness Index (CI): A Physically Grounded Scalar Measure of Conscious Degree, Structure, and Evolutionary Potential. BFUT P21. Zenodo. DOI: 10.5281/zenodo.20025739

[3] Sharma, V. S. (2026). Black Holes as Central Gravitational Vortices Lacking Singularities: The Universal Centrality Rule. BFUT P6. Zenodo. DOI: 10.5281/zenodo.19300874

[4] Hameroff, S., & Penrose, R. (2014). Consciousness in the universe: A review of the Orch-

OR theory. Physics of Life Reviews, 11(1), 39-78.

[5] Weinberg, S. (1989). The cosmological constant problem. Reviews of Modern Physics, 61(1), 1.

[6] Godel, K. (1949). An example of a new type of cosmological solutions. Reviews of Modern Physics, 21(3), 447.

[7] Gross, D. J., & Wilczek, F. (1973). Ultraviolet behavior of non-Abelian gauge theories. Physical Review Letters, 30(26), 1343.

[8] Politzer, H. D. (1973). Reliable perturbative results for strong interactions? Physical Review Letters, 30(26), 1346.

[9] Ritz, T., et al. (2000). A model for photoreceptor-based magnetoreception in birds. Biophysical Journal, 78(2), 707-718.

[10] Rauch, H., et al. (1975). Verification of coherent spinor rotation of fermions. Physics Letters A, 54(6), 425-427.

[11] Werner, S. A., Colella, R., Overhauser, A. W., & Eagen, C. F. (1975). Observation of the phase shift of a neutron due to precession in a magnetic field. Physical Review Letters, 35(16), 1053-1055.

[12] ATLAS Collaboration (2012). Observation of a new boson at a mass of 125 GeV. Physics Letters B, 716(1), 1-29.

[13] CMS Collaboration (2012). Observation of a new boson at a mass of 125 GeV. Physics Letters B, 716(1), 30-61.

[14] Higgs, P. W. (1964). Broken symmetries and the masses of gauge bosons. Physical Review Letters, 13(16), 508-509.

[15] Feynman, R. P., Leighton, R. B., and Sands, M. (1965). The Feynman Lectures on Physics, Volume III, Chapter 6 (Spin One-Half). Addison-Wesley.

[16] Pauli, W. (1925). Ueber den Zusammenhang des Abschlusses der Elektronengruppen im Atom mit der Komplexstruktur der Spektren. Zeitschrift fuer Physik, 31, 765-783. DOI: 10.0967/BF02980631

[17] Pauli, W. (1940). The connection between spin and statistics. Physical Review, 58(8), 716-722. DOI: 10.1103/PhysRev.58.716

[18] Penrose, R. (2004). The Road to Reality: A Complete Guide to the Laws of the Universe. Jonathan Cape.

[19] Gerlach, W., and Stern, O. (1922). Der experimentelle Nachweis der Richtungsquantelung im Magnetfeld. Zeitschrift fuer Physik, 9, 349-352. DOI: 10.0967/BF01326983

[20] Feynman, R. P. (1986). The reason for antiparticles. In R. P. Feynman and S. Weinberg, Elementary Particles and the Laws of Physics: The 1986 Dirac Memorial Lectures. Cambridge University Press.

[21] Sharma, V. S. (2026). Cosmic Rotation Across Scales, Emergent Orbital Hierarchy, and the Large-Scale Challenge to Metric Expansion. BFUT P9. Zenodo. DOI: 10.5281/zenodo.19341549

[P16A] Sharma, V. S. (2026). Antimatter, Annihilation, and the Stability Filter: Predictions for the CERN Antihydrogen Programme. BFUT P16A. Zenodo. DOI: 10.5281/zenodo.20201014